INL/RPT-23-72875

Thermal Spectrum Molten Salt-Fueled Reactor Reference Plant Model

July 2023

Mustafa K. Jaradat[1] and Javier Ortensi[1]

[1]*Reactor Physics Methods and Analysis*

INL is a U.S. Department of Energy National Laboratory
operated by Batelle Energy Alliance, LLC

INL/RPT-23-72875

Thermal Spectrum Molten Salt-Fueled Reactor Reference Plant Model

Mustafa K. Jaradat[1] **and Javier Ortensi**[1]

[1]**Reactor Physics Methods and Analysis**

July 2023

Idaho National Laboratory
Nuclear Science and Technology
Idaho Falls, Idaho 83415

http://www.inl.gov

Prepared for the
Office of Nuclear Regulatory Research
U. S. Nuclear Regulatory Commission
Washington, D. C. 20555
Task Order No.: 31310019F0015

Page intentionally left blank

SUMMARY

This report details a fully coupled neutronics thermal hydraulics reference plant model for a thermal spectrum molten salt-fueled reactor.

The multiphysics model is developed on the Nuclear Regulatory Commission's Comprehensive Reactor Analysis Bundle available on the Idaho National Laboratory high-performance computer, which natively and seamlessly couples Griffin and SAM codes of the Multiphysics Object-Oriented Simulation Environment (MOOSE)-based applications. Griffin provides the reactor physics capabilities, k-eigenvalue, delayed neutron precursor concentrations, and transient solutions for stationary and flowing fuels. SAM provides the solution of mass, momentum, and energy conservation equations of the whole system with a set of system components for one-dimensional single-phase flow. The neutronics feedback model relies primarily on fuel and moderator temperatures, fuel salt density, and delayed neutron precursors distributions. This report presents our results for the coupled steady state core and an unprotected loss of flow event. Although this model is prototypical regarding capabilities in the Comprehensive Reactor Analysis Bundle, its results are consistent with experimental data of the pump transient tests that were performed at zero power of the Molten Salt Reactor Experiment (MSRE).

ACKNOWLEDGEMENTS

This research made use of the resources provided by the Nuclear Energy Advanced Modeling and Simulation program managed by the Department of Energy Office of Nuclear Energy.

This research made use of the resources of the High Performance Computing Center at Idaho National Laboratory, which is supported by the Office of Nuclear Energy of the U.S. Department of Energy and the Nuclear Science User Facilities under Contract No. DE-AC07-05ID14517.

Description of the various author roles:

- Mustafa Jaradat—conceptual development, cross sections, neutronics model development, and multiphysics analysis
- Javier Ortensi—conceptual development, multiphysics analysis

This work would not have been possible without the contributions from the Idaho National Laboratory Griffin development team: Yaqi Wang, Sebastian Schunert, and Olin Calvin.

We are grateful to SAM developers team for providing the thermal hydraulics model of the molten salt reactor experiment that is used in this work, including Gang Yang and Ling Zou.

Page intentionally left blank

CONTENTS

SUMMARY iii

ACKNOWLEDGMENT iv

1 INTRODUCTION 1

2 REACTOR DESIGN DESCRIPTION 2

3 ANALYSIS METHODOLOGY 6

3.1 Reactor Physics Methods 6

3.1.1 Multigroup Cross Section Generation Procedure 6
3.1.2 Neutronics Methods 8
3.2 Thermal Fluids Methods 10

4 MODEL DESCRIPTION 12

4.1 Neutronics Model 12

4.2 Thermal-Hydraulics Model 13

4.3 Multiphysics Core Model 15

4.4 Assumptions and Limitations 15

5 RESULTS 18

5.1 Cross Sections Audit 18

5.2 Multiphysics Steady State Solution 20

5.3 Validation Tests 25

5.4 Unprotected Loss of Flow Transient 28

5.4.1 Full Power Case 29
5.4.2 Zero Power Case 30

6 CONCLUSIONS 36

7 FUTURE WORK 37

REFERENCES 39

FIGURES

Figure 1. Schematic diagram of MSRE reactor systems. 2
Figure 2. MSRE reactor assembly (top) and lattice made of graphite with half of four fuel salt channels (bottom). 5
Figure 3. Developed OpenMC model for MSRE multigroup cross sections generation. 7
Figure 4. Developed model for neutronics calculation. 13
Figure 5. Developed model for thermal fluids calculations using SAM. 14
Figure 6. Coupling scheme for Multiphysics core calculations of MSRE using Griffin and SAM 16
Figure 7. Comparison of the isothermal temperature feedback coefficient calculated by OpenMC and Griffin. 19
Figure 8. Steady state delayed neutron precursor distributions calculated by SAM. 22
Figure 9. Steady state delayed neutron precursor distributions used in Griffin calculations. . 23
Figure 10. Steady state neutronic distributions of (left to right) power density, fast, epithermal, and thermal neutron flux (see Table 10). 24
Figure 11. Steady state thermal fluid distributions of (left to right) fuel salt temperature, solid temperature, porosity, superficial velocity magnitude, and intrinsic velocity magnitude (see Eqs. 7-9). 24
Figure 12. Control rod axial position during pump start-up and coast down tests. 27
Figure 13. Comparison calculated reactivity losses by Griffin/SAM and measured values data during pump start-up and coast down tests. 27
Figure 14. The MSRE ULOF transient at full power (a) power, average fuel and moderator temperatures, (b) inlet flow rate, inlet and outlet fuel temperatures. 32
Figure 15. Fuel salt temperature field during ULOF at full power. 33
Figure 16. DNP group 3 distribution during ULOF at full power. 34
Figure 17. The MSRE ULOF transient at zero power (a) power, average fuel and moderator temperatures, (b) inlet flow rate, inlet and outlet fuel temperatures. 35

TABLES

Table 1. List of deliverables and tasks. 1
Table 2. MSRE core specifications. 3
Table 3. Fuel salt specifications. 4
Table 4. Fuel salt and graphite thermophysical properties. 4
Table 5. Neutron energy group boundaries for the 16 group structure. 8
Table 6. Comparison of eigenvalue and leakage fraction of OpenMC and Griffin models. 18
Table 7. Comparison of calculated feedback coefficients by OpenMC and Griffin. 19
Table 8. Drift of DNP impact on eigenvalue and reactivity. 21
Table 9. Kintecs parameters of MSRE stationary and flowing fuels. 21
Table 10. Fission fraction in MSRE core regions and energy range. 21
Table 11. Sequence of events for the protected pump start-up and coast-down. 26
Table 12. Sequence of events of the ULOF accident. 28

ACRONYMS

ANL	Argonne National Laboratory
DNP	delayed neutron precursor
DNPs	delayed neutron precursors
INL	Idaho National Laboratory
MOOSE	Multiphysics Object-Oriented Simulation Environment
MSR	Molten Salt Reactor
MSRE	Molten Salt Reactor Experiment
MSRs	Molten Salt Reactors
NRC	Nuclear Regulatory Commission
ORNL	Oak Ridge National Laboratory
SAM	System Analysis Module
SOW	statement of work
ULOF	Unprotected Loss Of Flow

Page intentionally left blank

1. INTRODUCTION

This report details the progress and activities of Idaho National Laboratory (INL) in regard to the Nuclear Regulatory Commission (NRC) project "Development and Modeling Support for Advanced Non-Light Water Reactors."

Table 1 provides a summary of completed tasks documented in this report to support the development of a reference plant model for analysis of a molten salt-fueled reactor (thermal spectrum). The table matches the deliverable number, statement of work (SOW) task, and (short) description of the deliverable. This report is organized as in the following: Section 2 provides a brief design description of the Molten Salt Reactor Experiment (MSRE) and fuel salt specifications. Section 3 discusses the cross section generation procedure, and the neutronics and thermal-hydraulics methods and analysis methodology used in this work. In Section 4, the developed Multiphysics models of the MSRE are described, and Section 5 presents the results of the steady state core, pump start-up and coast down validation tests, and the Unprotected Loss Of Flow (ULOF) transient at zero and full power cases. Finally, the summary and future work are provided in Section 6 and Section 7.

Table 1: List of deliverables and tasks.

Deliverable Number	SOW Task	Description
14	14a	Develop a coupled Molten Salt Reactor Experiment (MSRE) model based on a simplified MSRE System Analysis Module (SAM) model that will be provided by the NRC.
14	14b	Simulate two transient cases, loss of forced flow transients with neutronic feedback effects and analyze the results.
14	14c	Prepare a summary letter describing the model and summarizing the results; and present the model and results to NRC.
14	14d	Develop macroscopic and microscopic cross-sections as needed.
18	18	Partial requirement for Task 18 "Prepare a report presenting and discussing the models and results developed under Task 14".

2. REACTOR DESIGN DESCRIPTION

Molten Salt Reactors (MSRs) with flowing fuel have the unique feature of utilizing the fuel salt for heat generation and extraction at the same time, where the fuel salt is circulating through the whole primary loop. This movement of fuel salt results in a partial decay of the delayed neutron precursors (DNPs) outside the core and the corresponding redistribution of the DNPs in the active region of the core. To capture this effect, neutronics and thermal-hydraulics tools need to be modified to handle such an effect [1–4]. INL is actively working on developing the neutronics and thermal-hydraulics tools to model the MSRs with flowing fuel. As one of the efforts, the neutronics code Griffin has been extended to handle the flowing fuel involving the drift of DNPs [5, 6]. In this work, a Multiphysics analyses of the Molten Salt Reactor Experiment (MSRE) are performed to verify the MSR capabilities and validate the code against available experimental data. A schematic diagram of the MSRE reactor systems is shown in Figure 1 [7].

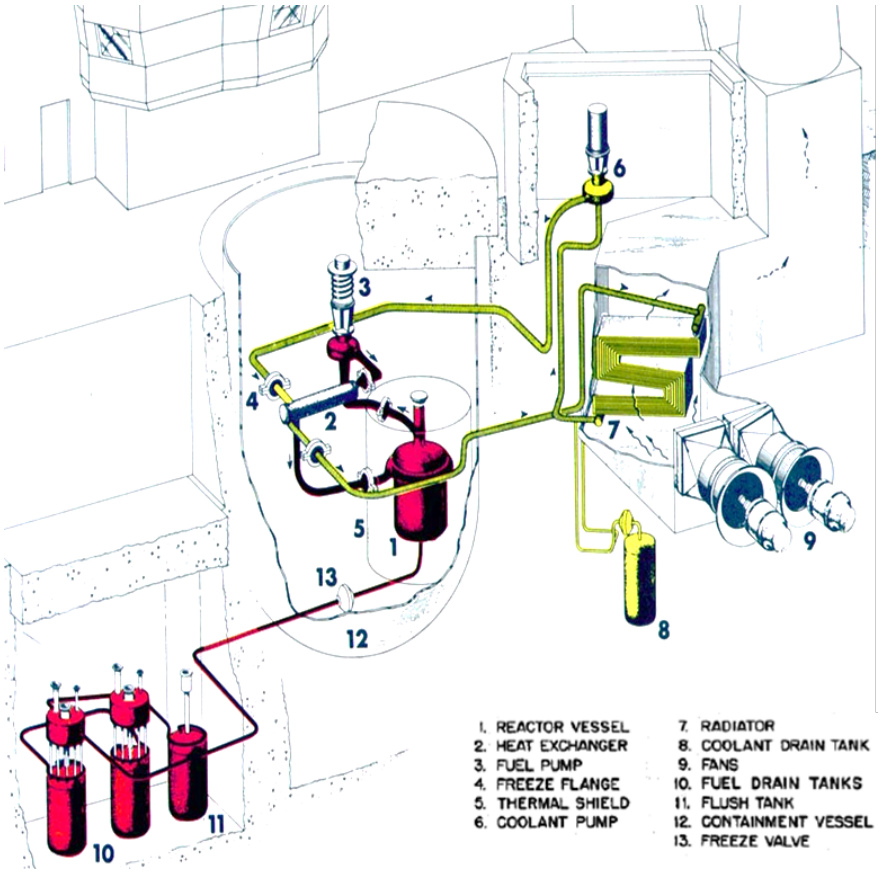

Figure 1: Schematic diagram of MSRE reactor systems.

The MSRE was built in 1964 at Oak Ridge National Laboratory (ORNL) to be the first reactor designed and operated with liquid fuel and moderated with graphite. The main purpose of the MSRE was to demonstrate the practicality of the liquid fuel operation at high temperatures and ensure the safety and reliability for developing the full-scale breeder MSR project [8, 9]. The total operation period of the MSRE was about 10 years, which provided the only source of experimental data regarding MSRs for validating the developed tools for MSRs analysis. The MSRE utilized a thermal neutron spectrum by allowing the liquid fuel salt to flow into graphite moderator channels. The reactor was initially operated with U-235 fuel, which was later replaced with U-233 fuel [10, 11]. The reactor main characteristics are provided in Table 2 [12–14].

Table 2: MSRE core specifications.

Parameter	Value
Design Core Power [MWth]	10.00
Core Height [m]	1.39
Core Diameter [m]	1.63
Fuel Salt Composition	LiF-BeF_2-ZrF_4-UF_4
Fuel Salt Molar Mass [%]	65.0-29.1-5.0-0.9
Fuel Enrichment [%]	33.0
Core Inlet temperature [K]	908.0
Core Outlet temperature [K]	936.0
Fuel Circulation Time [s]	25.2

The MSRE lattice was made of vertical graphite stringers with a 5.08 cm x 5.08 cm cross section. The fuel salt flows through a rectangular channel of 3.05 cm x 1.016 cm with round corners of radius 0.508 cm in the sides of the stringers [13]. The MSRE core configuration is shown in Figure 2, the top figure shows the MSRE reactor assembly [10], while the bottom figure shows the MSRE 4-halfs fuel salt channels with graphite stringer. The liquid fuel salt is composed of LiF-BeF_2-ZrF_4-UF_4, the atomic fractions of the fuel salt isotopes are provided in Table 3 [12, 14]. The thermophysical properties of the fuel salt and solid moderator is provided in Table 4 [15]. These data were collected from several design and analysis reports of the MSRE.

Table 3: Fuel salt specifications.

Isotope	Atom Fraction
Li-7	2.63371E-01
F-19	5.94814E-01
Be-9	1.17909E-01
U-235	1.20340E-03
U-238	2.44327E-03
Zr-90	1.04234E-02
Zr-91	2.27310E-03
Zr-92	3.47447E-03
Zr-94	3.52107E-03
Zr-96	5.67260E-04

Table 4: Fuel salt and graphite thermophysical properties.

Parameter	Value
Fuel Salt	
Density [kg/m^3]	ρ [T]= 2263-0.4798x(T[K]-923.0)
Density [@ 922.0 K]	2263.5
Thermal Conductivity [W/m·K]	1.4
Specific Heat [J/kg·K]	1868.0
Dynamic Viscosity [Pa·s]	0.263371
Graphite	
Density [kg/m^3]	1860.0
Thermal Conductivity [W/m·K]	40.1
Specific Heat [J/kg·K]	1757.3

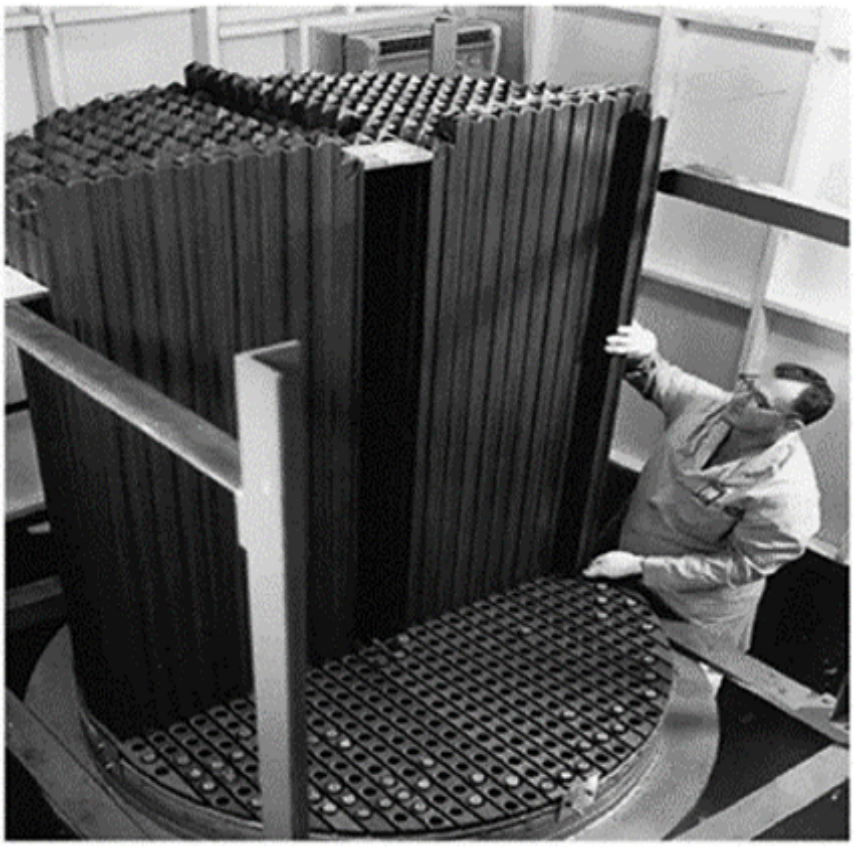

(a) Reactor assembly

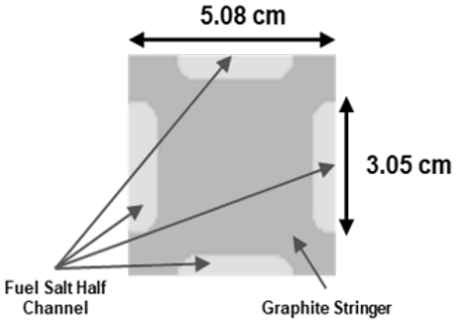

(b) Lattice

Figure 2: MSRE reactor assembly (top) and lattice made of graphite with half of four fuel salt channels (bottom).

3. ANALYSIS METHODOLOGY

In this work, a multiphysics reference plant model of the MSRE was developed using the Multiphysics Object-Oriented Simulation Environment (MOOSE) [16–18] framework. The multiphysics model consists of three models coupled using the MultiApp system: (1) Griffin neutronics model, (2) SAM core thermal-hydraulics model, and (3) SAM outer loop thermal-hydraulics model. Section 3.1 briefly introduces the reactor physics methods used in this work, while the thermal-hydraulics methodology is described in Section 3.2.

3.1 Reactor Physics Methods

Griffin is a reactor multiphysics application built on MOOSE and is based on the technology developed for Rattlesnake [19], Mammoth [20], and PROTEUS [21]. Griffin provides neutron transport, delayed neutron precursor distribution for flowing fuel, depletion, core performance, decay heat, and cross section calculation capabilities for non-light-water advanced reactor technologies. In this work, Griffin's diffusion approximation was used to solve the linearized Boltzmann transport equation with the multigroup approximation in the energy domain. In order to perform neutronics calculations with Griffin, multigroup cross sections need to be provided as a function of reactor state parameters, such as temperature and density. For MSRE analysis, the multi-group cross sections were generated using OpenMC code [22] as discussed in the following subsection.

3.1.1 Multigroup Cross Section Generation Procedure

To model heterogeneous geometry of the MSRE core and to account for the spectral changes in generating cross sections, the Monte Carlo code OpenMC [22] was used to generate multigroup cross sections. A full 3-D core model was developed for MSRE using the OpenMC code to generate multigroup microscopic cross sections and to verify the Griffin steady state model considering a stationary fuel without thermal feedback. The OpenMC model of the MSRE was adopted from [3, 23]. Also, the multigroup energy structure and the number of groups used to generate cross sections were selected based on a previous study [23] that was performed to optimize the energy group structure and the number of groups. In this work, a 16 energy group structure was utilized

to generate multigroup cross sections at several fuel salt and moderator temperatures with ENDF-VII.1 neutron data [24]. The 16 energy group structure is provided in Table 5 [23].

The MSRE cross sections were generated considering isothermal temperatures of the fuel salt and the solid moderator ranging between 860 K–1000 K. The temperature tabulation points were 860, 880, 900, 908, 922, 936, 960, 980, and 1000 K. The cross sections were prepared for 3 regions: Homogeneous core (fuel salt and graphite), upper and lower plena, and considering a fresh fuel composition and including delayed neutron data, as discussed in [3, 23]. The core was divided into several regions in the radial and axial directions to capture the neutron spectral changes at different core zones due to large leakage fraction. Figure 3 shows the developed OpenMC full core model of the MSRE.

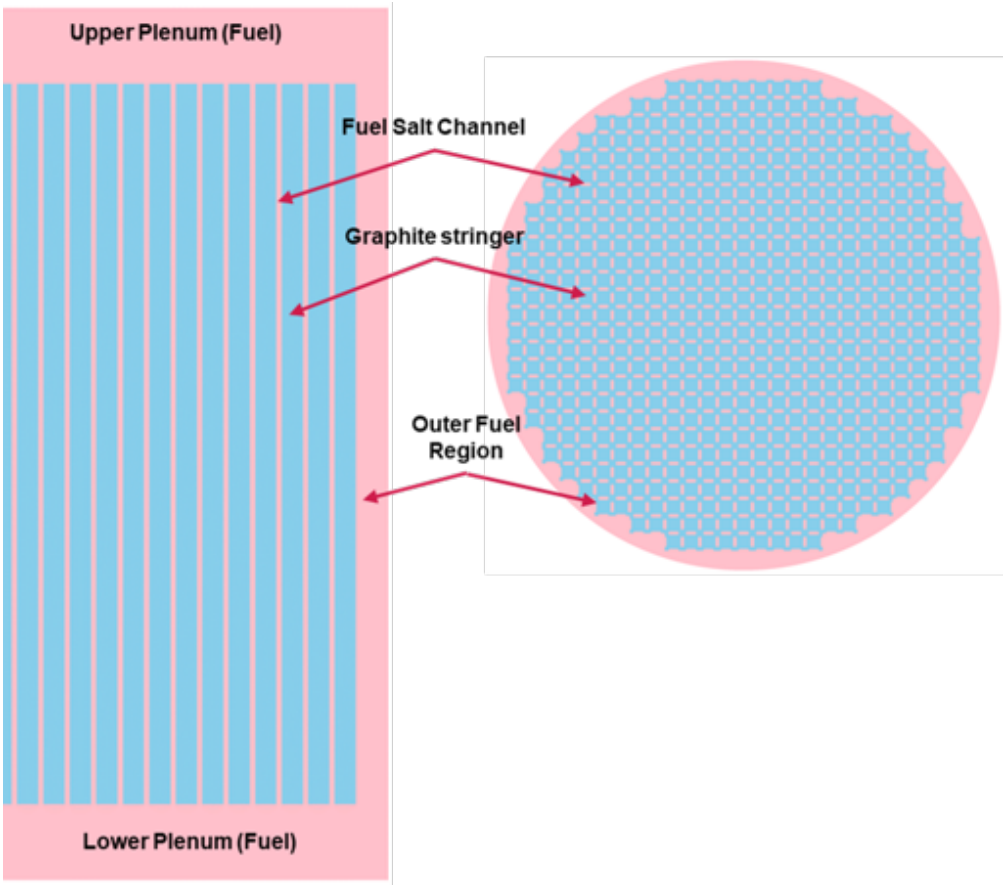

Figure 3: Developed OpenMC model for MSRE multigroup cross sections generation.

Table 5: Neutron energy group boundaries for the 16 group structure.

Group	Energy [eV]		Group	Energy [eV]	
	Upper	Lower		Upper	Lower
1	2.00E+07	3.68E+06	9	1.30E+00	6.25E-01
2	3.68E+06	1.35E+06	10	6.25E-01	4.00E-01
3	1.35E+06	5.00E+05	11	4.00E-01	2.50E-01
4	5.00E+05	6.73E+04	12	2.50E-01	1.80E-01
5	6.73E+04	9.12E+03	13	1.80E-01	1.40E-01
6	9.12E+03	1.49E+02	14	1.40E-01	8.00E-02
7	1.49E+02	4.00E+00	15	8.00E-02	4.20E-02
8	4.00E+00	1.30E+00	16	4.20E-02	1.00E-04

3.1.2 Neutronics Methods

Legacy neutronics solvers are well developed for solid stationary fuels. However, liquid flowing fuel reactors as in MSRs need special treatment to handle the drift of the DNPs and to calculate the proper delayed neutron source. For stationary fuels, the delayed neutrons are produced at the same location where the fission reaction occurred. Typically, in steady state calculations, the prompt and delayed fission neutron sources are represented with a single total fission neutron source. While in MSRs with flowing fuel, the delayed neutron source must be calculated separately to account for the flow effects on the redistribution of the DNPs and their decay outside the core region which requires solving the DNP equations including a drift term to account for the flow effects. For time-dependent calculations, the prompt and delayed fission sources are calculated separately to account for the delay in the fission products decay and the production of the delayed neutrons by solving the time-dependent DNP equations at each time point with the additional advection term.

In this work, Griffin is used to model the MSRE with flowing fuel using its diffusion solver which has the capability to model MSRs with flowing fuel. Griffin can solve the DNP equations with an advection term given the velocity field of the fuel salt and the residence time in the outer loop to account for the decay of DNPs and proper calculation of the inlet boundary condition. Also, Griffin can calculate the delayed neutron source given the DNP distributions calculated externally by species transport code such as SAM, as discussed in the following section.

Considering flowing fuel, the multigroup time-dependent diffusion equation for the neutron

flux and the DNP equations are given in Equation 1 and Equation 2, respectively, as

$$\begin{aligned}\frac{1}{v_g}\frac{\partial \phi_g(\vec{r},t)}{\partial t} - \nabla \cdot D_g(\vec{r},t)\nabla\phi_g(\vec{r},t) + \Sigma_{tg}(\vec{r},t)\phi_g(\vec{r},t) = \sum_{g\prime=1}^{G}\Sigma_{sg\prime g}(\vec{r},t)\phi_{g\prime}(\vec{r},t) \\ + \frac{(1-\beta)\chi_{pg}(\vec{r},t)}{k_{eff}}\sum_{g\prime=1}^{G}\nu\Sigma_{fg\prime}(\vec{r},t)\phi_{g}\prime(\vec{r},t) + \sum_{k=1}^{K}\chi_{dkg}(\vec{r},t)\lambda_k C_k(\vec{r},t), \qquad g = 1,2,.....,G,\end{aligned} \tag{1}$$

$$\frac{\partial C_k(\vec{r},t)}{\partial t} + \nabla\cdot(\vec{u}(\vec{r},t)C_k(\vec{r},t)) + \lambda_k C_k(\vec{r},t) = \frac{\beta_k}{k_{eff}}\sum_{g\prime=1}^{G}\nu\Sigma_{fg\prime}(\vec{r},t)\phi_{g}\prime(\vec{r},t), \qquad k = 1,2,.....,K, \tag{2}$$

where u is the fuel velocity and the other notations are conventional. The term $\nabla\cdot(\vec{u}(\vec{r},t)C_k(\vec{r},t))$ in Equation 2 accounts for the drift of the DNPs at time t and position $\vec{r}$. In steady state calculations, the time derivatives are omitted from Equations 1 and 2, and both equations are solved to obtain the total neutron source (prompt and delayed) and calculate effective multiplication factor (k_{eff}) of the system.

To calculate the kinetics parameters of the system, the adjoint flux solution must be used as weighting function and it should be calculated in advance. For stationary fuel the definition of the effective delayed neutron fraction β_{eff} and neutron mean generation time Λ can be given by

$$\beta_{eff}^{static} = \frac{<\phi^*, \chi_{dk}\sum_{k=1}^{K}\beta_k(\nu\Sigma_f\phi)>}{<\phi^*, \chi(\nu\Sigma_f\phi)>}, \tag{3}$$

$$\Lambda^{static} = \frac{<\phi^*, (v^{-1}\phi)>}{<\phi^*, \chi(\nu\Sigma_f\phi)>}. \tag{4}$$

For flowing fuel, the definition of the kinetics parameters is slightly different as provided in Equations 5 and 6 for effective delayed neutron fraction and mean generation time, respectively [25]. To compute the kinetics parameters for flowing fuel, the adjoint solution of the neutron flux and the the DNPs must be calculated. The solution of the adjoint DNP equations requires modifications of the neutron diffusion and DNP equations which is discussed in details in Reference [3, 23].

$$\beta_{eff}^{flowing} = \frac{< \phi^*, \sum_{k=1}^{K} (\chi_{dk} \lambda_k C_k) >}{< \phi^*, (1-\beta)\chi_p(\Sigma_f \phi) > + < \phi^*, \sum_{k=1}^{K} (\chi_{dk} \lambda_k C_k) >}, \tag{5}$$

$$\Lambda^{flowing} = \frac{< \phi^*, (v^{-1}\phi) >}{< \phi^*, (1-\beta)\chi_p(\Sigma_f \phi) > + < \phi^*, \sum_{k=1}^{K} (\chi_{dk} \lambda_k C_k) >}. \tag{6}$$

The delayed neutron losses β_{eff}^{losses} due to the drift of DNPs can be computed simply by subtracting the $\beta_{eff}^{flowing}$ from β_{eff}^{static}. In Griffin, the capability of calculating kinetics parameters for flowing fuel is not ready yet, but it is planned to be added in the next fiscal year. Instead, the delayed neutron losses are computed simply from static calculations of the reactivity changes at different core states.

3.2 Thermal Fluids Methods

The SAM [26] is an analysis tool being developed at Argonne National Laboratory (ANL) that focuses on modeling advanced reactor concepts distinguished with single-phase, low-pressure, and high-temperature. SAM has a whole-plant transient analysis capability with a set of system components, such as heat exchangers, pumps, and pipes. SAM was initially developed to model the one-dimensional (1-D) single-phase flow. [Recently, a multi-dimensional (Multi-D) flow capability has been developed to consider both the general multi-dimensional flow model and the porous medium-based flow model]. The porous medium model was used in this work to represent the MSRE core region. Equations 7, 8, and 9 show the porous media mass, momentum, and energy conservation equations, respectively, which are then solved using a finite-element discretization scheme. The fluid and solid energy conservation equations are handled distinctly and are coupled through a heat transfer coefficient. As a result, the solid temperature field must be solved to fully define the system. This solution is based on the solid energy conservation equation seen in Equation 10, which includes internal heat generation to take into account the heat produced within the solid moderator for the MSR case.

$$\frac{\partial \epsilon \rho_f}{\partial t} + \nabla \cdot (\epsilon \rho_f \vec{v}) = 0, \tag{7}$$

$$\rho_f \frac{\partial \vec{v}}{\partial t} + \frac{\rho_f}{\epsilon}(\vec{v} \cdot \nabla)\vec{v} + \epsilon \nabla p - \epsilon \rho_f \vec{g} + W \rho_f \vec{v} = 0, \tag{8}$$

$$\epsilon\rho_f C_{p,f}\frac{\partial T_f}{\partial t} + \epsilon\rho_f C_{p,f}\nabla\vec{v}\cdot(T_f) - \nabla\cdot(\epsilon\kappa_f\nabla T_f) + \alpha(T_f - T_s) = \dot{q}'''_f, \tag{9}$$

$$(1-\epsilon)\rho_s C_{p,s}\frac{\partial T_s}{\partial t} - \nabla\cdot(\kappa_s\nabla T_s) + \alpha(T_s - T_f) = \dot{q}'''_s, \tag{10}$$

where ϵ is the porosity of the medium, $\epsilon\vec{v}$ is the superficial velocity, $\vec{v}$ is the real or intrinsic velocity, and the subscripts f and s denote the liquid and solid phases, respectively.

SAM also has additional capability to model mass transport of species with advection through the system. This is applicable to the transport of the delayed neutron precursors (DNPs) given the delayed fission source for MSRs. To model DNPs transport in the system, SAM solves the passive scalar equation for DNPs transport given the delayed neutron source and decay constant of each delayed neutron family or groups as:

$$\epsilon\rho_f\frac{\partial C_k}{\partial t} + \epsilon\vec{v}\rho_f\nabla C_k - \epsilon\rho_f D\nabla^2 C_k + \epsilon\rho_f\lambda_k C_k = S_k, \qquad k = 1, 2, ..., K, \tag{11}$$

where C_k is the delayed neutron precursor (DNP) of family k, S_k is the delayed neutron fission source of group k, and D is the salt diffusion coefficient which is related to Schmidt number S_c to account for turbulent diffusivity of the salt. Schmidt number has a typical value of 0.85 and it can be defined as:

$$S_c = \frac{\mu}{\rho D} \tag{12}$$

where ρ and μ are the salt density and dynamic viscosity, respectively.

The unit of the DNPs calculated by Equation 11 is precursor per unit mass and porosity. However, the value used to perform neutronics calculations must be in unit of precursor per unit volume. Proper conversion of units is required to preserve the quantities. The validity of using the porous media approximation for MSRs analysis which handles the liquid salt and solid moderator as a single homogeneous region is questionable and requires many verification and validation tests.

4. MODEL DESCRIPTION

A description of the developed MSRE models that covers various physics relevant to the performance of the steady state and transient calculations is provided in this section. Section 4.1 describes the main neutronics model parameters and geometry. Then, the thermal fluid models of the core and outer loop are discussed in Section 4.2. Finally, the MOOSE Multiphysics coupling model is discussed in Section 4.3 followed by main assumptions and limitations.

4.1 Neutronics Model

The MSRE neutronics model was developed considering a 2-D axisymmetric domain in R-Z coordinate using the multigroup diffusion approximation to the linearized Boltzmann transport equation. To account for the effect of the DNPs drift and their decay in the outer loop, the DNP distributions are obtained from thermal-hydraulic calculations and used to construct the total neutron source.

Several simplifications were made to the MSRE reactor geometry to perform the simulation and analysis efficiently. The core configuration was developed by neglecting the control rods and the outside regions of the active core, including the core container, the downcomer, the reactor vessel, the gap between reactor vessel and insulator, the insulator, and the thermal shield.

The core region has a radius of 0.70485 m and the heights of the lower plenum, core, and upper plenum are 0.12954 m, 1.6637 m, and 0.21336 m, respectively. The lower and upper plenum contain only fuel salt. While the core region was considered as a homogeneous mixture of the fuel salt and the graphite moderator with ratio of 0.2229 to 0.7771 in volume, respectively. The material properties were taken from the available data in the MSRE reports published by ORNL.

The R–Z geometry model of the MSRE was selected to perform the steady state and transient analysis because it represents the outer regions of the core accurately by preserving the reaction rates and leakage fraction compared to relative Monte Carlo solution. The 16-energy groups structure was selected to perform the analysis because it provided the smallest difference in eigenvalue and leakage fraction of the tested cases as discussed in Reference [23]. The developed neutronics model of the MSRE was divided into three regions: core (regions 1 to 4), and lower plenum and upper plenum (region 5) as shown in Figure 4.

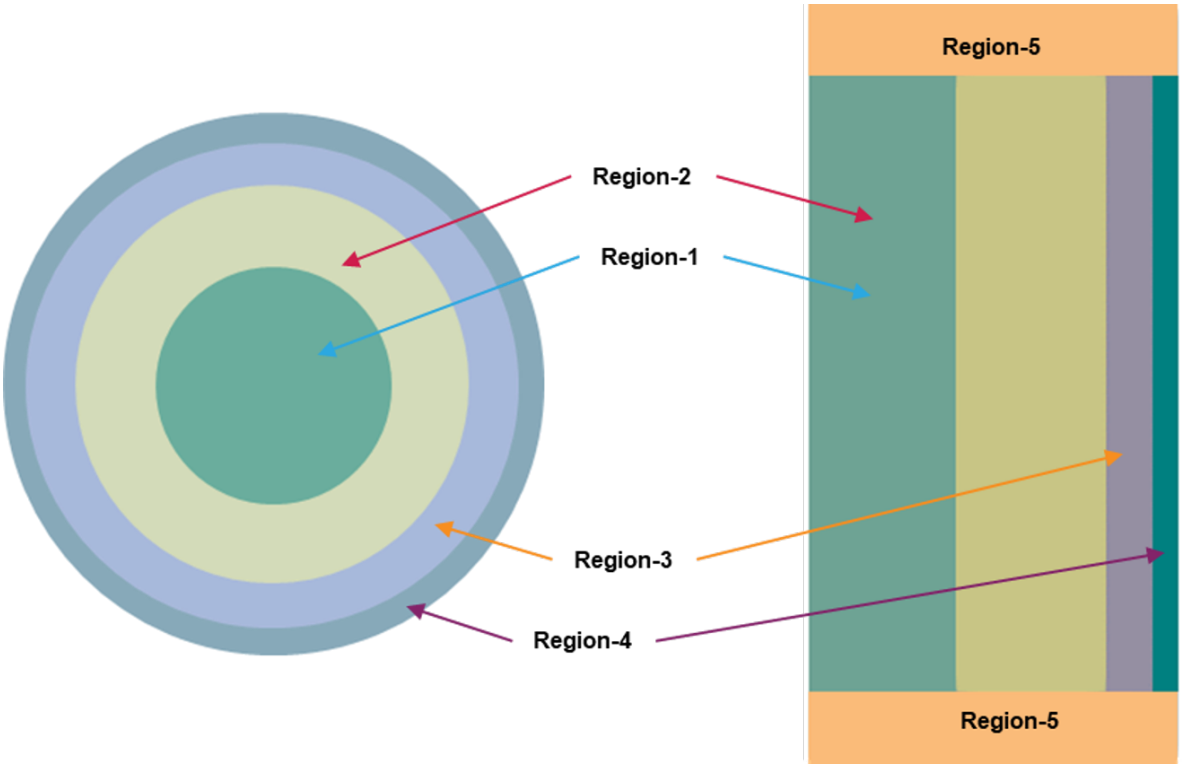

Figure 4: Developed model for neutronics calculation.

4.2 Thermal-Hydraulics Model

The thermal-hydraulics model of the MSRE, developed using the SAM code by Argonne National Laboratory (ANL), is adopted in this work. The model is discussed in detail in Reference [27]. In this model, the core region is represented by a 2-D porous media approximation and the outer loop is modeled with 1-D/0-D fluid channels to solve the mass momentum and energy equations along with the DNP equations to account for the drift of the DNPs within the core and its decay in the outer loop.

A 2-D axisymmetric domain in R-Z geometry is developed to model the MSRE core and includes the lower plenum, core, and upper plenum with height of 0.12954 m, 1.6637 m, and 0.21336 m, respectively. The porosity of the core and plenum are set to 0.2228 and 1.0, respectively. Also, the model simplifies the geometry of the upper plenum with a cylindrical shape instead of the curved shape to ensure convergence of the solution during the loss of flow transient where the slat velocity is reduced to a very low level. The volumes of the core and plenum were adjusted to preserve the total volume of the fuel salt in the reactor ignoring the solid structures in the plenum.

To ensure axial flow of the salt in the graphite stringers, constraints are placed on the radial velocity of the core and lower plenum to suppress the lateral movement.

The external loop is modeled with 1-D/0-D fluid components that include the primary pump, heat exchanger, connecting pipes, and downcomer. The 2-D core region is coupled with the outer loop using 0-D components at the downcomer outlet and the core outlet pipe to connect the two domains at the boundaries. A shell-and-tube type heat exchanger was used and all the connecting pipes have a diameter of 0.127 m. The thermophysical properties of fuel salt and the graphite utilized in this model are modified as described in Table 4. Figure 5 shows the developed model for the thermal fluids core region with the outer loop model.

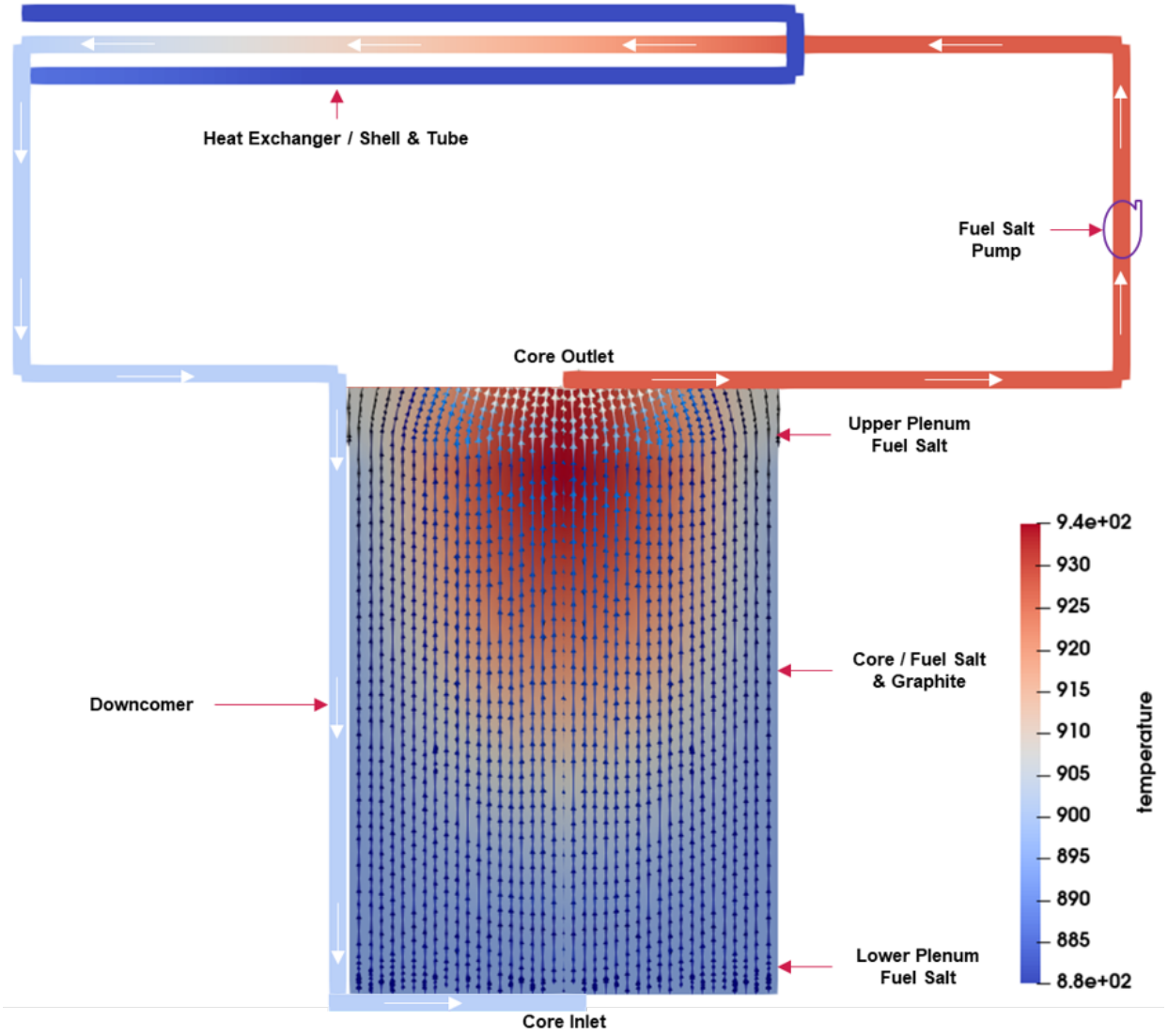

Figure 5: Developed model for thermal fluids calculations using SAM.

The DNP equations are solved using the scalar transport capability of SAM to account for their decay in the outer loop accurately. The fuel salt enters the core through the lower plenum and flows into the core and and exits the upper plenum to the outer loop pipes and flow through the primary pump, heat exchanger, and downcomer before the fuel salt reenters the lower plenum. The total circulation time of the fuel salt is about 25 s. The pump head was adjusted to sustain the flow circulation time with a core inlet velocity of 0.05 m/s.

4.3 Multiphysics Core Model

The developed Multiphysics model of the MSRE consists of three components: (1) Griffin neutronics model, (2) SAM multi-D core model, and (3) SAM 1-D outer loop model. Griffin is considered the main-app while SAM multi-D is considered a sub-app. Also, SAM 1-D is called as a sub-app of SAM multi-D.

The parameters needed by each model component to obtain a Multiphysics coupled solution are transferred between model components at each calculation point or time step. Figure 6 shows the coupling scheme and the transferred parameters between the main-app and the sub-apps. Griffin provides the power density and fission source distributions to SAM Multi-D. The power density distribution is used to obtain fuel and moderator temperatures, density, pressure, and velocity fields. While the fission source distribution is used to calculate the DNPs distribution. SAM multi-D and 1-D models exchange parameters at the downcomer outlet and the top core outlet pipe to obtain core inlet temperature, density, pressure, temperature, and DNP values. The fuel salt and moderator temperatures and densities are transferred to Griffin from SAM to update the cross sections and the fuel salt isotopic densities for proper feedback calculations. Also, the DNPs is transferred to determine the delayed neutron source and construct the total fission neutron source in the core region considering their decay in the outer loop.

4.4 Assumptions and Limitations

The following assumptions and limitations are applicable to the developed neutronics model:

- A 2-D RZ representation of the reactor core is used, and it provides a reasonable representation of the reactor geometry.

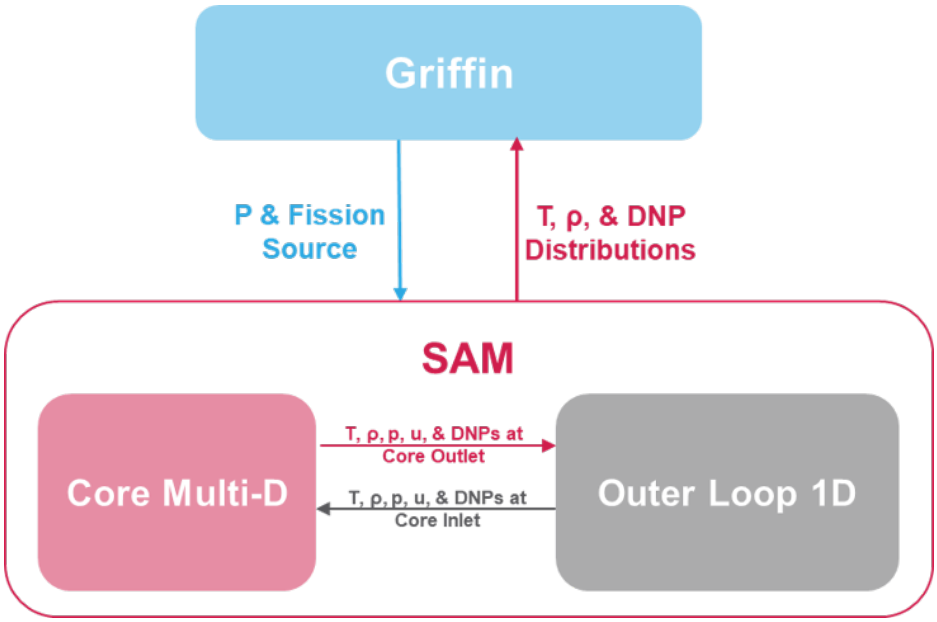

Figure 6: Coupling scheme for Multiphysics core calculations of MSRE using Griffin and SAM

- The multigroup neutron diffusion equation provides a flux solution of the core and reflector regions that is accurate enough for core calculations.
- The microscopic cross sections are functionalized considering the fuel salt and moderator temperatures implicitly taking into account density changes in isotopic format.
- The core region is considered as a homogeneous mixture of the fuel salt and the graphite stringers with a fuel salt fraction of 0.2228.
- The control rods are omitted from the current model which need to be considered in future improvements.
- The model is limited to the core region without considering the outer structure regions of the core barrel, reactor vessel, and outer reactor regions which need to be considered in future improvements.
- The atom densities of the fuel salt are adjusted to match the salt expansion and the relevant changes in the salt density as the temperature changes.
- The expansion of the solid graphite is not considered in the current model and it is assumed to have minimal impact on the calculations.

- The geometry of the upper plenum is considered as a simplified cylindrical shape instead of the curved shape to accommodate the same mesh utilized in the thermal-hydraulics model.
- The DNP distributions are provided as an external source obtained from thermal-hydraulic calculations and used to construct the total neutron source.
- The delayed neutron losses are calculated form the reactivity changes of stationary and flowing fuel cases.

The assumptions and limitations applicable to the developed thermal fluids model are that:

- The thermal fluid model of the core is represented by a 2-D porous region to capture most of the important effects in the core.
- The outer loop and external core components are modeled with 1-D/0-D fluid channels.
- The heat generated in graphite due to neutron slowing down and gamma heating is not considered.
- The geometry of the upper plenum is considered as simplified cylindrical shape instead of the curved shape.
- The volumes of the upper plenum and lower plenum are adjusted to preserve the total salt volume in the reactor.
- The porosity in the core assembly is set to 0.2228 and 1.0 in the upper and lower plenum.
- The solid structures in the upper and lower plenum are ignored.
- Constraints are placed on the radial velocity of the core and lower plenum to suppress the lateral movement and to ensure vertical/axial flow of the salt in the graphite stringers.
- A centrifugal pump is utilized in the outer loop with the head adjusted to sustain the flow circulation with a velocity of 0.05 m/s at the core inlet.
- The 2-D core region and 1-D outer loop are coupled with 0-D components at the downcomer outlet and the top core outlet pipe.

5. RESULTS

The results of the MSRE initial core steady state and transient solutions are discussed in this section along with validation test results against available experimental data of the MSRE obtained from open literature. Section 5.1 discusses the cross sections generated with the full core model in OpenMC with verification tests of the Griffin model against OpenMC reference solutions for stationary fuel to ensure that all values are within acceptable limits. Section 5.2 presents the steady state Multiphysics solution of the MSRE core. In Section 5.3, validation transient test results of the pump start-up and coast down tests are presented followed by the results of the Unprotected Loss Of Flow (ULOF) transient scenario at full and zero power cases as discussed in Section 5.4.

5.1 Cross Sections Audit

The multigroup cross sections generated with OpenMC and used in Griffin were tested and compared to the reference OpenMC results at different temperatures as provided in Table 6, where the eigenvalue and the leakage fractions are compared at inlet, outlet, and average core temperatures of the fuel salt. The difference in eigenvalue and leakage fraction are within 150 pcm and 0.2%, respectively. Also, Table 7 provides the values of the fuel, moderator, and isothermal temperature coefficients calculated by OpenMC and Griffin. The maximum difference in the temperature coefficients are within 0.3 pcm/K (4.0%). Figure 7 shows a comparison of the MSRE isothermal temperature coefficient calculated by OpenMC and Griffin with the temperature range of 860 K to 1000 K.

Table 6: Comparison of eigenvalue and leakage fraction of OpenMC and Griffin models.

Temp. [K]	OpenMC		Griffin (Diff.)	
	k_{eff}	Leakage	k_{eff} (pcm)	Leakage (% Rel. Diff.)
908	1.06504	0.33497	74.9	-0.191
922	1.06294	0.33600	138.7	-0.154
936	1.06103	0.33703	99.0	-0.180

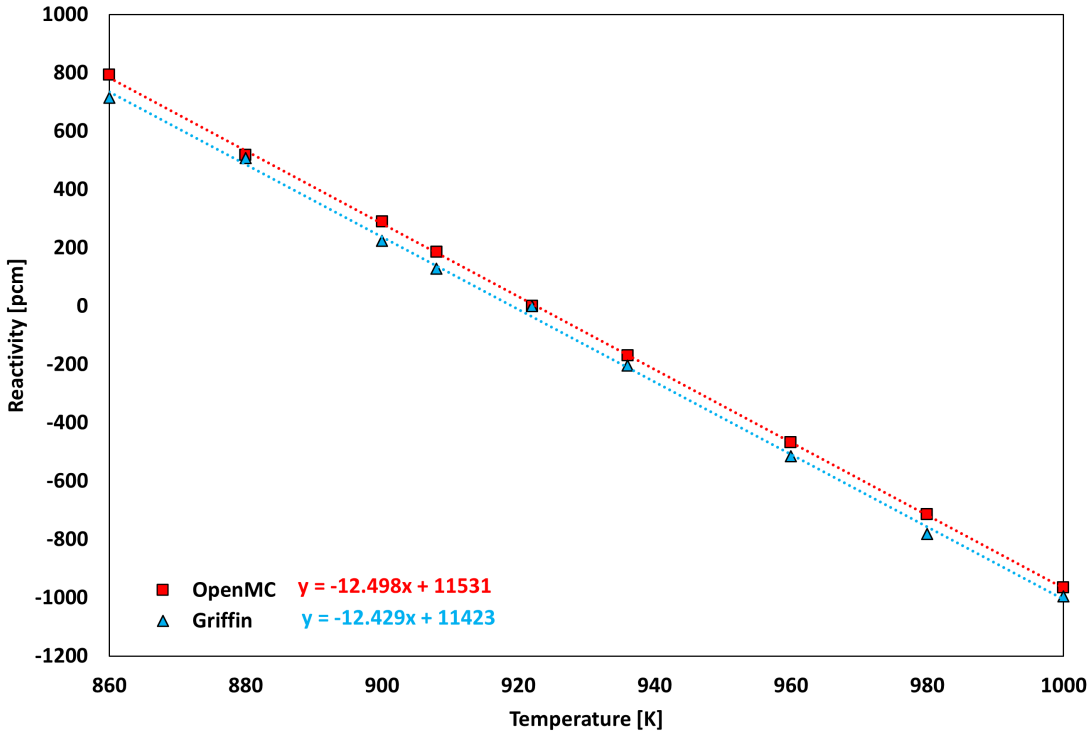

Figure 7: Comparison of the isothermal temperature feedback coefficient calculated by OpenMC and Griffin.

Table 7: Comparison of calculated feedback coefficients by OpenMC and Griffin.

Feedback Coef. [pcm/K]	OpenMC	Griffin	Difference [%]
Isothermal	-12.5	-12.4	0.8
Fuel	-7.4	-7.1	4.1
Graphite	-5.1	-5.3	-3.9

5.2 Multiphysics Steady State Solution

This section presents the steady state calculation results of the MSRE simplified core. To demonstrate the impact of the DNPs drift on eigenvalue, several cases were considered with and without thermal feedback, delayed neutron source, and flow of the fuel salt in terms of reactivity change as presented in Table 8. The reactivity change was calculated relative to the case with delayed neutron source and without fuel salt flow. The delayed neutron contribution is about 670 pcm which is the value of the effective delayed neutron fraction (β_{eff}) of stationary fuel as given in Reference 9. The drift of the DNPs in the core, and its decay in the outer loop, results in roughly 240.0 pcm in reactivity losses. The effect of the thermal feedback on the reactivity change with delayed neutrons is minimal.

Table 9 provides the kinetics parameters of stationary and flowing fuel, and the losses in β_{eff} which is the difference between the β_{eff} of stationary and flowing fuel, and it is consistent with the value calculated by reactivity change of 242.0 pcm. The kinetics parameters were calculated from static calculations and utilizing the multi-app system. The measured value of the DNP losses for the MSRE is 212.0 pcm which is 30 pcm lower than the value calculated by the Multiphysics model of the MSRE developed in this work. In Figure 8, the distributions of the DNPs in the core region is shown for all groups as calculated by SAM code in units of precursor per unit mass and porosity. While Figure 9 shows the DNPs used in Griffin calculations in units of precursor per unit volume which is re-normalized to account for homogenization effect in the core region. The DNPs groups with longer half-life (smaller decay constant as in groups 1 and 2) have higher delayed neutron losses, and their distribution is shifted upward to the top of the core and peaks at the upper plenum region. While the DNPs groups with shorter half-life (larger decay constant in as group 6) have smaller delayed neutron losses and their distribution is similar to the power distribution and it peaks at the core center region.

To show the importance of the upper and lower plena in the neutronics calculations, specifically eigenvalue and fission neutron source, the fission fraction in the three core regions (moderated core, lower plenum, and upper plenum) is provided in Table 10 at different energy ranges. Both plena contribute about 12.0% of the total fission that comes from fast and epithermal energy ranges. Even though the neutron flux level is reduced significantly in these regions but the sub-

Table 8: Drift of DNP impact on eigenvalue and reactivity.

Case				k_{eff}	Reactivity
No.	Feedback	DNP	Fuel Flow		[pcm]
1	-	x	-	1.03834	0.0
2	-	-	-	1.03114	672.5
3	-	x	x	1.03574	241.7
4	x	x	-	1.03748	0.0
5	x	-	-	1.03028	673.2
6	x	x	x	1.03487	242.8

Table 9: Kintecs parameters of MSRE stationary and flowing fuels.

Group	$\lambda[s^{-1}]$	β_{eff} [pcm]		
		Stationary	Flowing	Losses
1	0.013	23.7	0.6	23.0
2	0.033	121.8	37.4	84.4
3	0.121	116.3	53.5	62.8
4	0.303	259.2	184.6	74.6
5	0.849	106.8	104.8	2.0
6	2.853	44.7	48.1	-3.4
Total	-	672.5	429.0	243.5
Mean Generation Time $\Lambda[ms]$			0.259	

stantial change in the volume of the fuel salt in these regions tends to increase the fission density.

Table 10: Fission fraction in MSRE core regions and energy range.

Energy Range	Fast	Epithermal	Thermal	All
Upper Energy	20.0 MeV	9.12 keV	0.625 eV	20.0 MeV
Lower Energy	9.12 keV	0.625 eV	1.0E-4 eV	1.0E-4 eV
Lower Plenum [%]	1.41	1.46	0.84	3.71
Active Core [%]	17.30	29.04	41.64	87.99
Upper Plenum [%]	3.33	3.65	1.33	8.31
Total [%]	22.04	34.15	43.80	100.00

Also, Figure 10 shows the distributions of the important neutronics parameters in the reactor core region, including power density, fast, epithermal, and thermal neutron fluxes. Figure 11 shows the distributions of the important thermal hydraulics parameters, including fuel salt and moderator temperatures, porosity, superficial and intrinsic velocity fields. The solutions of the field variables are as expected. The power peaks at the core center and small peaks are observed in the upper and lower plena due to massive change in the fuel salt volume as discussed earlier.

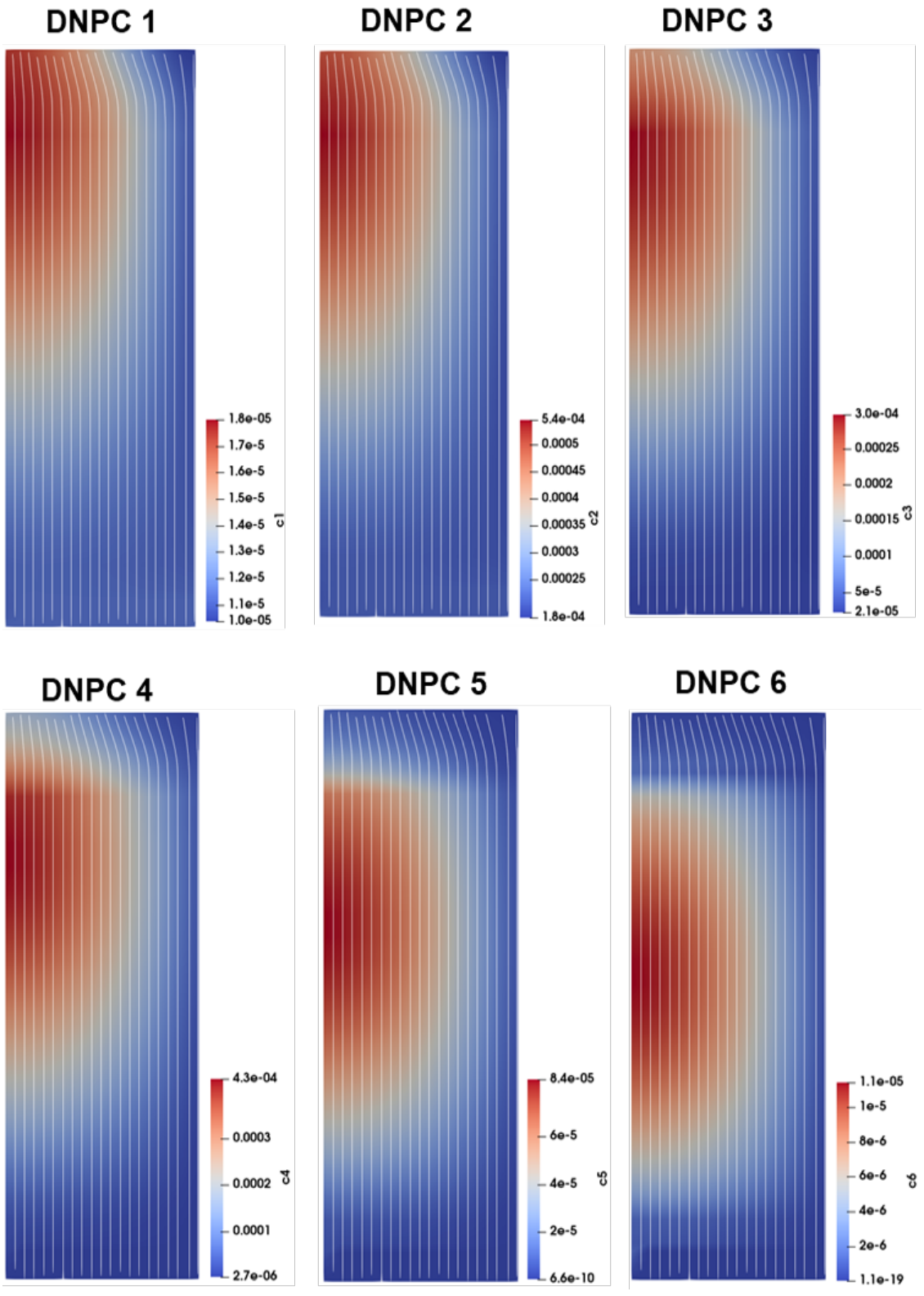

Figure 8: Steady state delayed neutron precursor distributions calculated by SAM.

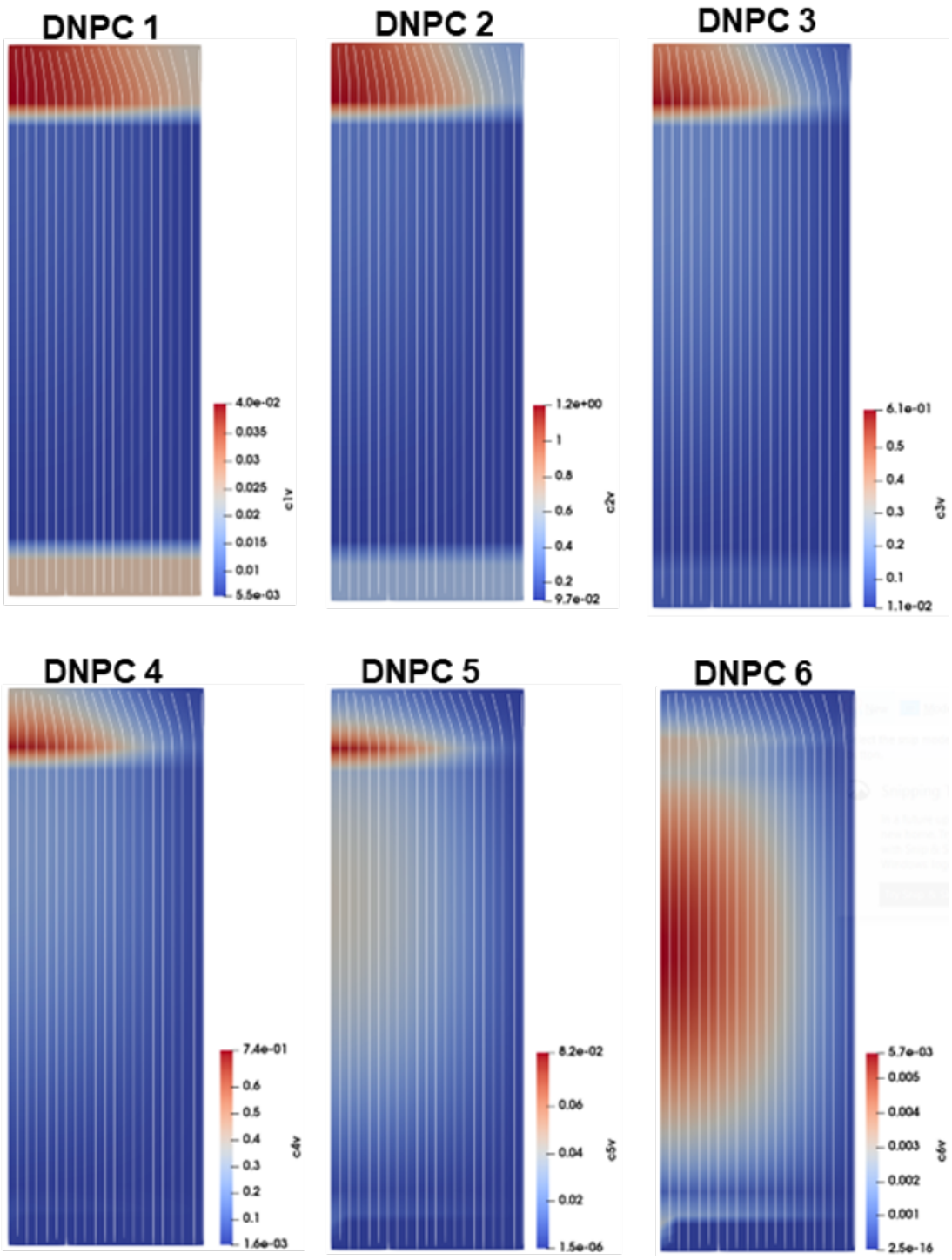

Figure 9: Steady state delayed neutron precursor distributions used in Griffin calculations.

The temperature fields are skewed to the upper core region with a maximum value of 950.0 K and an inlet salt temperature of 900.0 K. The velocity field and the formed streamlines are all in the axial direction with an inlet velocity of about 0.05 m/s and 0.2 m/s in the active core region.

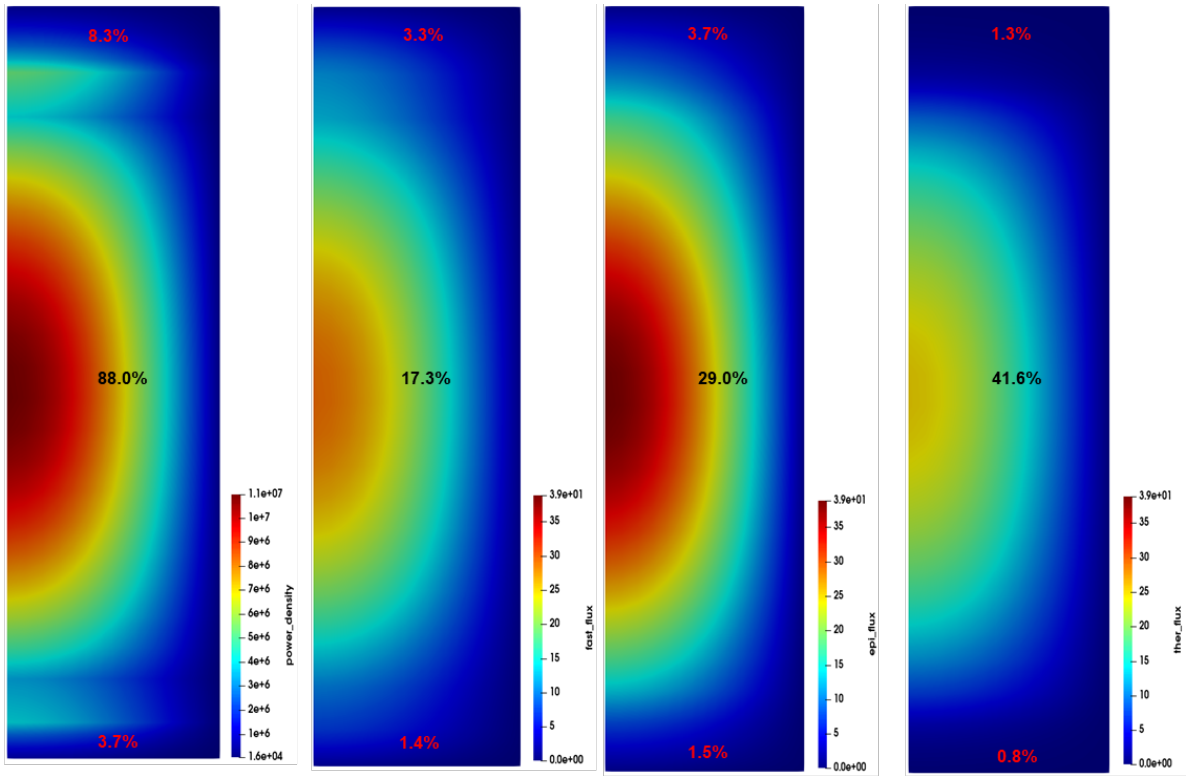

Figure 10: Steady state neutronic distributions of (left to right) power density, fast, epithermal, and thermal neutron flux (see Table 10).

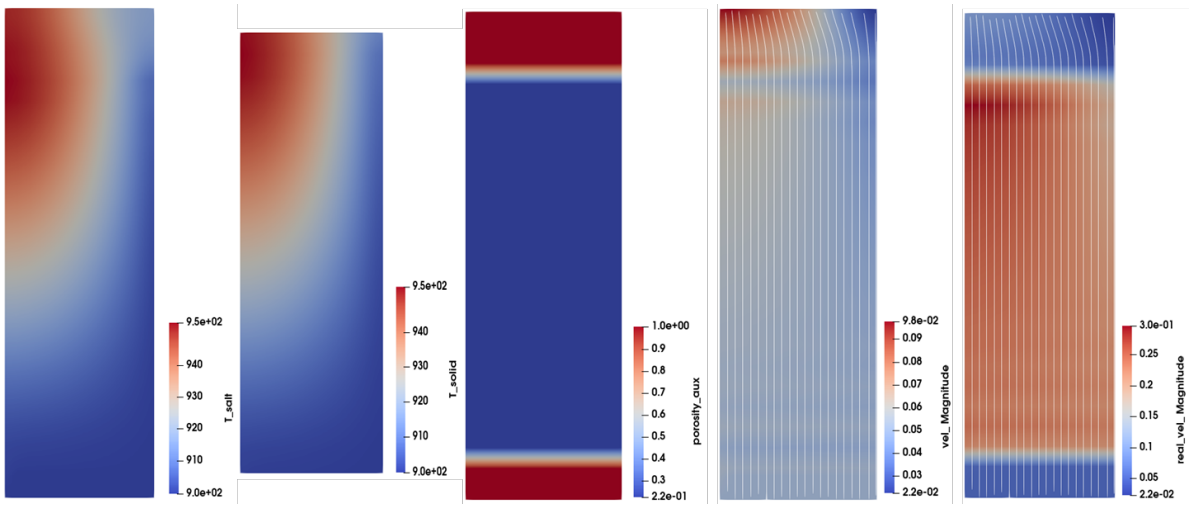

Figure 11: Steady state thermal fluid distributions of (left to right) fuel salt temperature, solid temperature, porosity, superficial velocity magnitude, and intrinsic velocity magnitude (see Eqs. 7-9).

5.3 Validation Tests

During the initial operation of the MSRE, several tests were performed at zero power before starting full power operation. Among these tests were the protected pump transient tests which were performed to evaluate the effects of flow rate changes on the reactivity during pump start-up and coast down transients. Also, a natural circulation test was performed to evaluate the feedback mechanism and to determine the characteristics of the heat removal of the system. In this section, validation test results of the Multiphysics MSRE model for pump start-up and coast-down tests are presented.

In the protected pump start-up and coast-down experiments, the reactor was fueled with $U-235$, and the reactor was operated at a low power level to ensure that the DNP losses were the only feedback mechanism. Initially, the equilibrium conditions of the system were established with minimal flow at the critical state. During the experiment, the fuel flow rate in the primary loop was increased or decreased by adjusting the primary pump head. The control rod positions were adjusted to maintain a constant low power and eliminate any thermal feedback effects. The control rod positions recorded during the pump start-up and coast-down experiments are shown in Figure 12 [13]. The control rod movement was compensating for the reactivity loss or gain due to the redistribution of the DNPs in the core and their decay outside the core. This decay is converted into reactivity data using the measured control rod worth curve which is equivalent to the reactivity perturbations of the fuel flow.

Multiphysics transient calculations were performed for the MSRE to simulate the pump start-up and coast down tests. Initial equilibrium conditions were established with minimal flow (about 0.01% of its nominal value) at zero power (0.01% of its full power). Both pump start-up and coast-down scenarios were simulated within the a same transient run. The sequence of events for both pump transients that are considered in performing the simulation are summarized in Table 11. In the pump start-up test, the fuel flow rate reached its nominal value in 10 s, while in the pump coast-down test it was decreased from its nominal value to zero in 15 s.

Figure 13 shows the a comparison of the reactivity losses calculated by the Multiphysics coupled model and the experimental values that was generated from converting the control rod position data into a reactivity data using measured control rod worth data for both pump transient

Table 11: Sequence of events for the protected pump start-up and coast-down.

Time [s]	Event
< 0	- Initial equilibrium conditions were established. - Salt pump head was set to 0.01% of its nominal value. - The power was maintained at 1.0 kW.
0	- Start increasing the pump head following the change in the mass flow of the experimental data.
0–10	- Start linearly increasing the pump head in the primary loop from 0.01% to 100.0% of its nominal value. - Maintain the reactor power at 1.0 kW.
10	- Primary loop pump start-up is completed.
10–400	- No change in input parameters.
400	- Start decreasing the pump head following the change in the mass flow of the experimental data.
400–415	- Start linearly decreasing the pump head in the primary loop from 100.0% to 0.01% of its nominal value. - Maintain the reactor power at 1.0 kW.
415	- Primary loop pump coast down is completed.
415–500	- No change in input parameters.
500	- Simulation end time.

tests. During the protected pump start-up test, the flow of fuel that starts outside the core leads to reactivity loss due to the decay of the DNPs outside the core and the losses increase with the increasing flow velocity which requires more control rod withdrawal to maintain criticality. The oscillatory behavior is observed due to un-decayed fuel flowing back and decays in the core region. The positive reactivity effect of the recirculated precursors entering the core is clearly seen 13 seconds after pump start-up. While in the protected pump coast-down transient, the reactivity increases with decreasing fuel flow rate due to the decay of the DNPs in the core region. Therefore, the compensated reactivity continues to decrease and reaches zero when all the precursors decay in the core which requires insertion of the control rod to maintain criticality. For both cases, the calculated values agree with measured values except for the pump start-up case where the oscillatory behaviour is slightly overestimated. This might be attributed to excluding the control rods from the current model and the simplifications that were made to perform this transient.

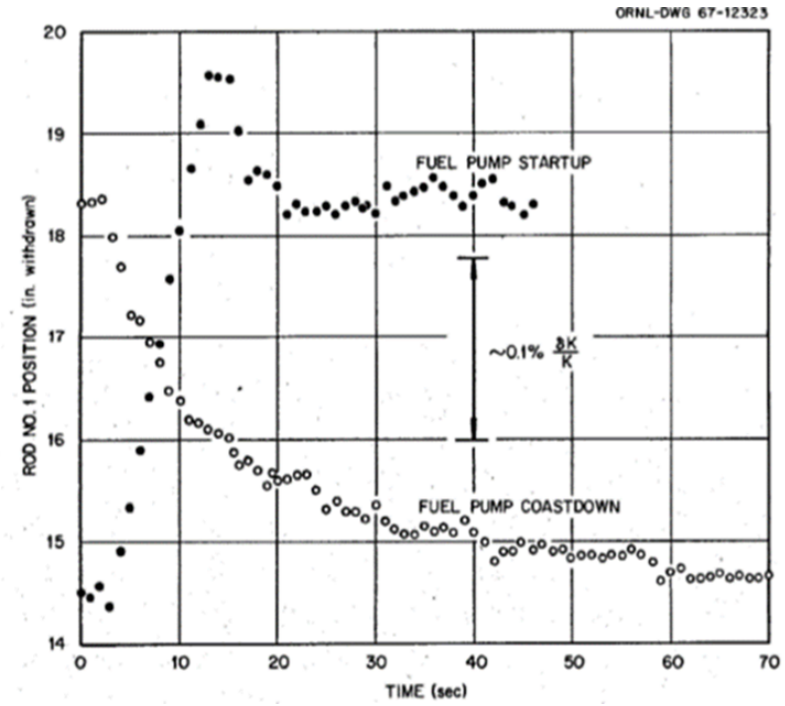

Figure 12: Control rod axial position during pump start-up and coast down tests.

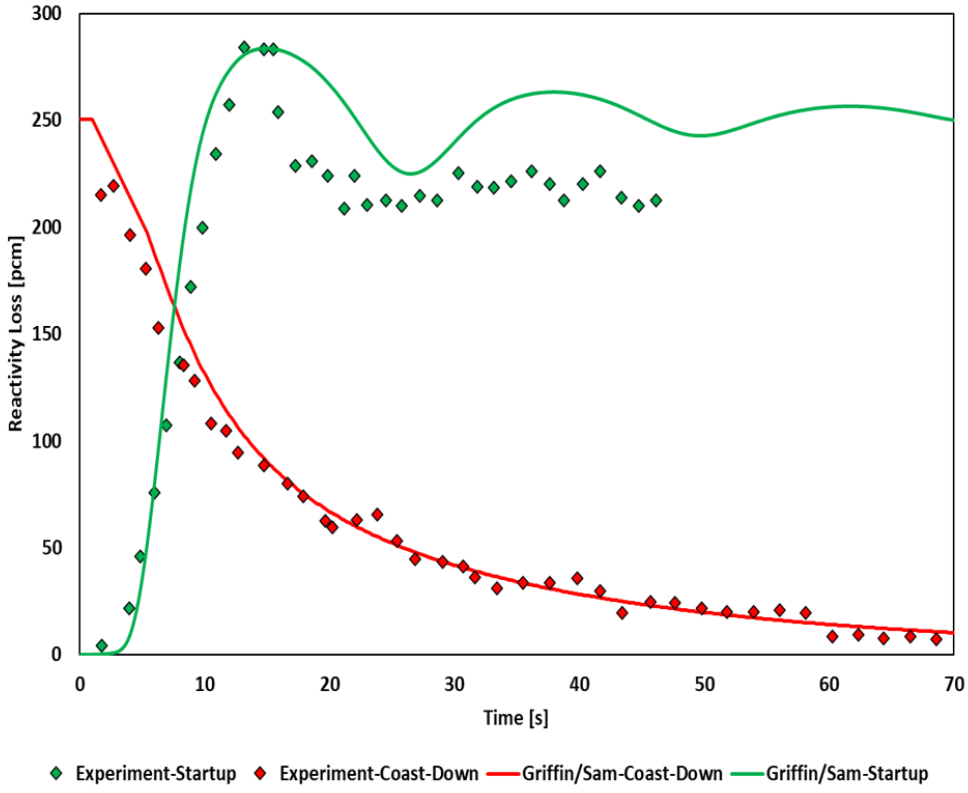

Figure 13: Comparison calculated reactivity losses by Griffin/SAM and measured values data during pump start-up and coast down tests.

5.4 Unprotected Loss of Flow Transient

The ULOF is one of the most important design basis accidents for MSRs. The reactivity feedback of MSRs has three main mechanisms: (a) the temperature effects through Doppler; (b) salt expansion or density changes; and (c) the flow of the fuel salt which results in DNPs losses and reactivity changes. At full power operation, the fuel temperature feedback is the dominant feedback mechanism while at low power operation, the flow rate change is the main feedback mechanism. To demonstrate the different feedback mechanisms and the impact of the DNPs during transient analysis, the ULOF of the MSRE core was simulated at full (100%) and zero (0.01%) power levels.

The ULOF accident scenario considered in this work assumes a complete loss of the primary cooling system while the secondary loop system remained operational for an initial core and therefore no decay heat was considered. Prior to the start of the transient, the steady state conditions were established by running a null transient. Then, the primary pump head was linearly reduced to reach the desired value. Beyond that point there were no changes in system input parameters. The sequence of events considered during ULOF accident is provided in Table 12.

Table 12: Sequence of events of the ULOF accident.

Time [s]	Event
< 0	- Steady state conditions for fresh core and flowing fuel were established. - Initial reactor power was set to 10 MWth (100%) in full power test. - Initial reactor power was set to 1 kWth (0.01%) in zero power test.
0–100	- Maintain steady state condition for the initial 100 s of the transient (null transient).
100	- Start of unprotected loss of flow accident assuming a complete power outage of the primary loop only.
100–130	- Start linearly reducing the pump head in the primary loop to 1.0% of its nominal value.
130	- Primary loop pump head ramp is completed.
130–4000	- No change in input parameters.
4000	- Simulation end time.

5.4.1 Full Power Case

To understand the power and temperature evolution during the ULOF transient, the transient was divided into three regions: (1) null transient; (2) power oscillation; and (3) thermal equilibrium regions. Figure 14 shows the total power and the average, maximum, inlet, and outlet temperatures of the fuel salt along with moderator temperatures and inlet flow rate of the salt for the MSRE ULOF transient at full power level. The following progression of the reactor total power and temperatures was observed during the full power ULOF transient:

- Region 1:
  - There was no change in input parameters of the system.
  - Confirm steady state conditions are well established for the first 100 s of the transient.
  - Reactor was operated at full power of 10 MWth and nominal flow rate was maintained.
- Region 2:
  - The transient was initiated and the fuel flow rate was linearly reduced to 1% of its nominal value in 30 s.
  - Following the flow reduction, the fuel salt temperature increases and it introduces a negative reactivity due to Doppler and salt expansion.
  - On the other hand, fuel salt velocity decreases and it introduces a positive reactivity due to the reduction in delayed neutron losses.
  - The negative temperature feedback is the dominant feedback mechanism, and the power starts decreasing.
  - Once the fuel salt is at the natural circulation level, the unheated salt starts flowing back into the core at slower rate, and the power increases again due to positive feedback of the reduced fuel temperature.
  - An oscillatory temperature behavior is observed due to the heat transferred to the graphite and extracted by the secondary system.
  - Similar power oscillations were observed opposing temperature oscillations due to thermal feedback effects.

- Region 3:
  - The power fluctuations decrease as the fuel salt and graphite achieve thermal equilibrium and the average temperature stabilizes at 930 K.
  - Power stabilizes at new level as the temperature fluctuations vanish which is about 45% of full power value.

Figures 15 and 16 show the fuel salt temperature field and the delayed neutron precursor distribution in the core region for delayed group 3 at different time points during the ULOF transient. The temperature distribution became significantly higher and more uniform at the top of the reactor due to reduced flow value and uniform and dissipation of the temperature through the solid graphite and heat extraction by the secondary system. The DNP distribution of group 3 (half-life of 5.74 s, $\lambda = 0.121\ s^{-1}$) tends to peak more in the core region as the transient progresses and the fuel salt flow reduced to the natural circulation level. This will reduce the delayed neutron losses due to decay outside the core, the magnitude of the DNP decreases due to decreased power and fission source. The other DNP groups follow the same behaviour more or less relative to their decay constants.

5.4.2 Zero Power Case

In MSRs, the zero power ULOF transient show a different side of the complicated physics that involve DNP distribution and their decay. Similar to the full power case, the power and temperature evolution during the ULOF transient at zero power level was divided into three regions. Figure 17 shows the total power and the average, maximum, inlet, and outlet temperatures of the fuel salt along with moderator temperatures and inlet flow rate of the salt for the MSRE ULOF transient at zero power level. The following progression of the reactor total power and temperatures was observed during the zero power ULOF transient:

- Region 1:
  - There was no change in input parameters of the system.
  - Confirm steady state conditions are well established for the first 100 s of the transient.
  - Reactor was operated at full power of 1 kWth and nominal flow rate was maintained.

- Region 2:
  - The transient was initiated and the fuel flow rate was linearly reduced to 1% of its nominal value in 30 s.
  - Following the flow reduction, the fuel salt velocity decreases which introduces positive reactivity due to the reduction in delayed neutron losses.
  - On the other hand, the fuel salt temperature increases which introduces negative reactivity due to Doppler and salt expansion.
  - The positive velocity feedback is the dominant feedback mechanism, and the power starts increasing and reaches its peak value at about 14% of its full power value which is 1400 times its initial value.
  - As a result, the fuel salt starts heating up as power increases which introduces a negative temperature feedback that became the dominate feedback mechanism after about 700 s and the power starts decreasing.
  - An oscillatory temperature behavior is observed due to the heat transferred to the graphite and extracted by the secondary system.
  - Similar power oscillations were observed opposing temperature oscillations due to thermal feedback effects.
- Region 3:
  - The power fluctuations decrease when fuel salt and graphite achieve thermal equilibrium and the average temperature stabilizes at 925 K.
  - Power stabilizes at new level as the temperature fluctuations vanish which is about 5% of full power value.

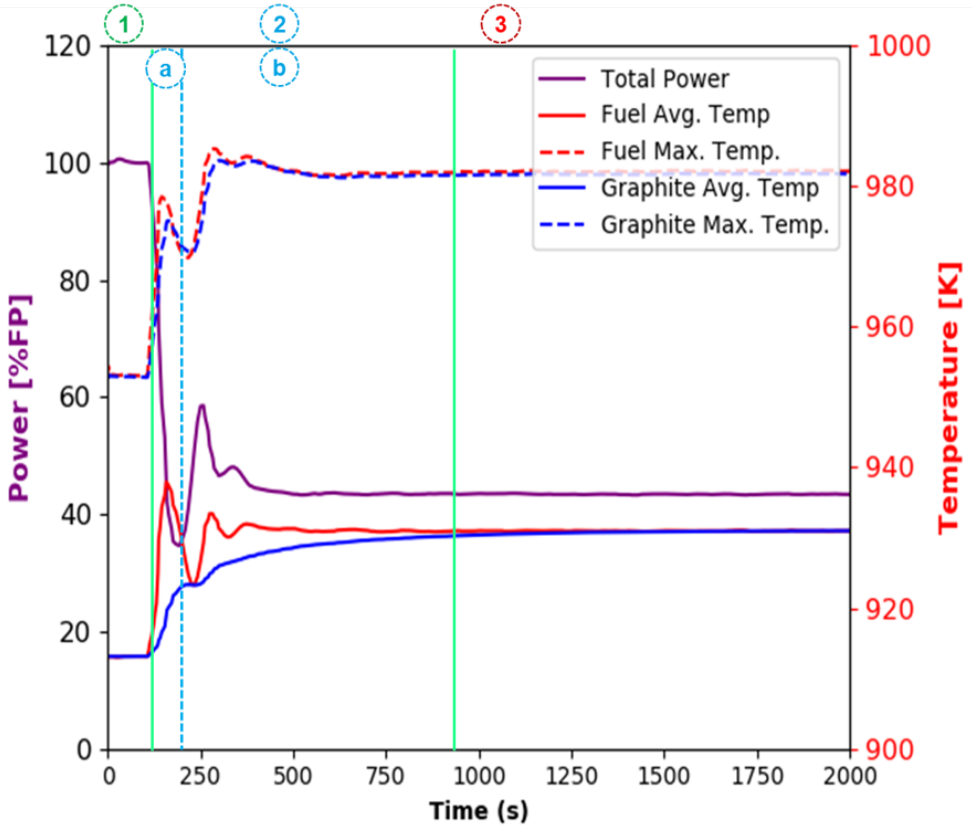

(a)

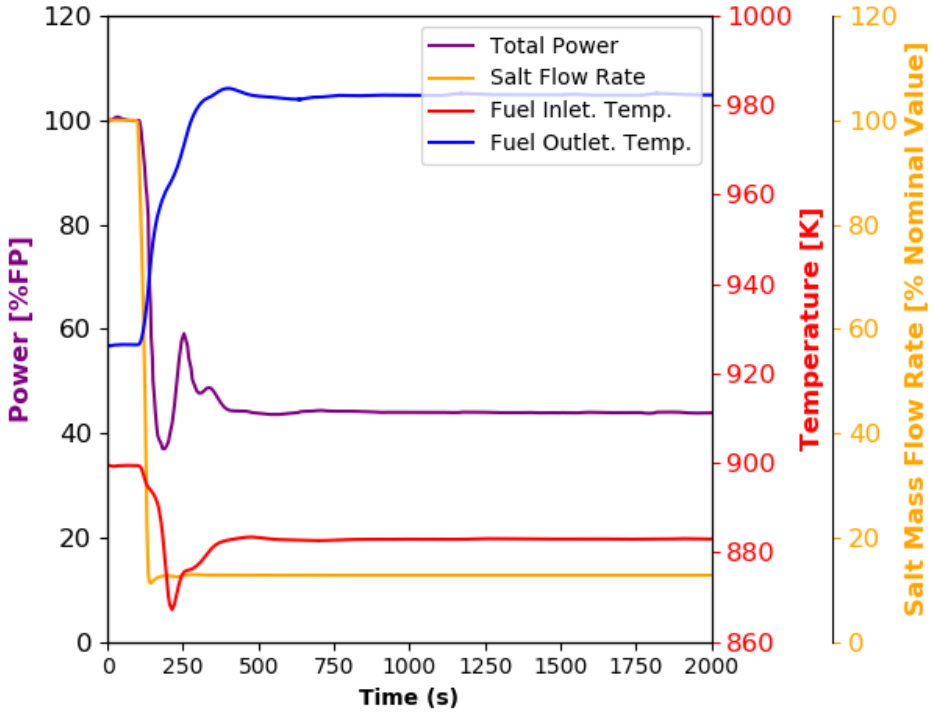

(b)

Figure 14: The MSRE ULOF transient at full power (a) power, average fuel and moderator temperatures, (b) inlet flow rate, inlet and outlet fuel temperatures.

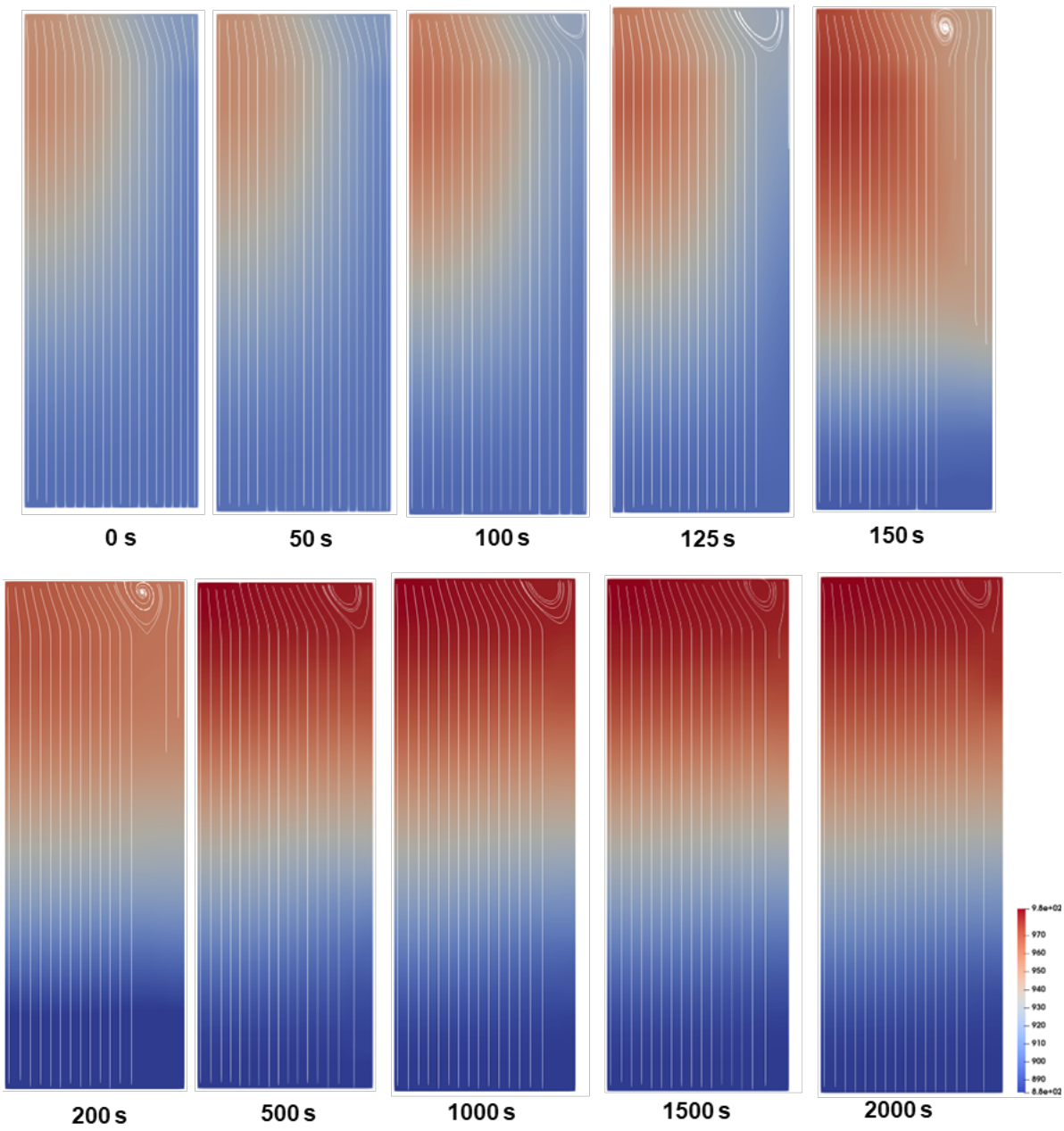

Figure 15: Fuel salt temperature field during ULOF at full power.

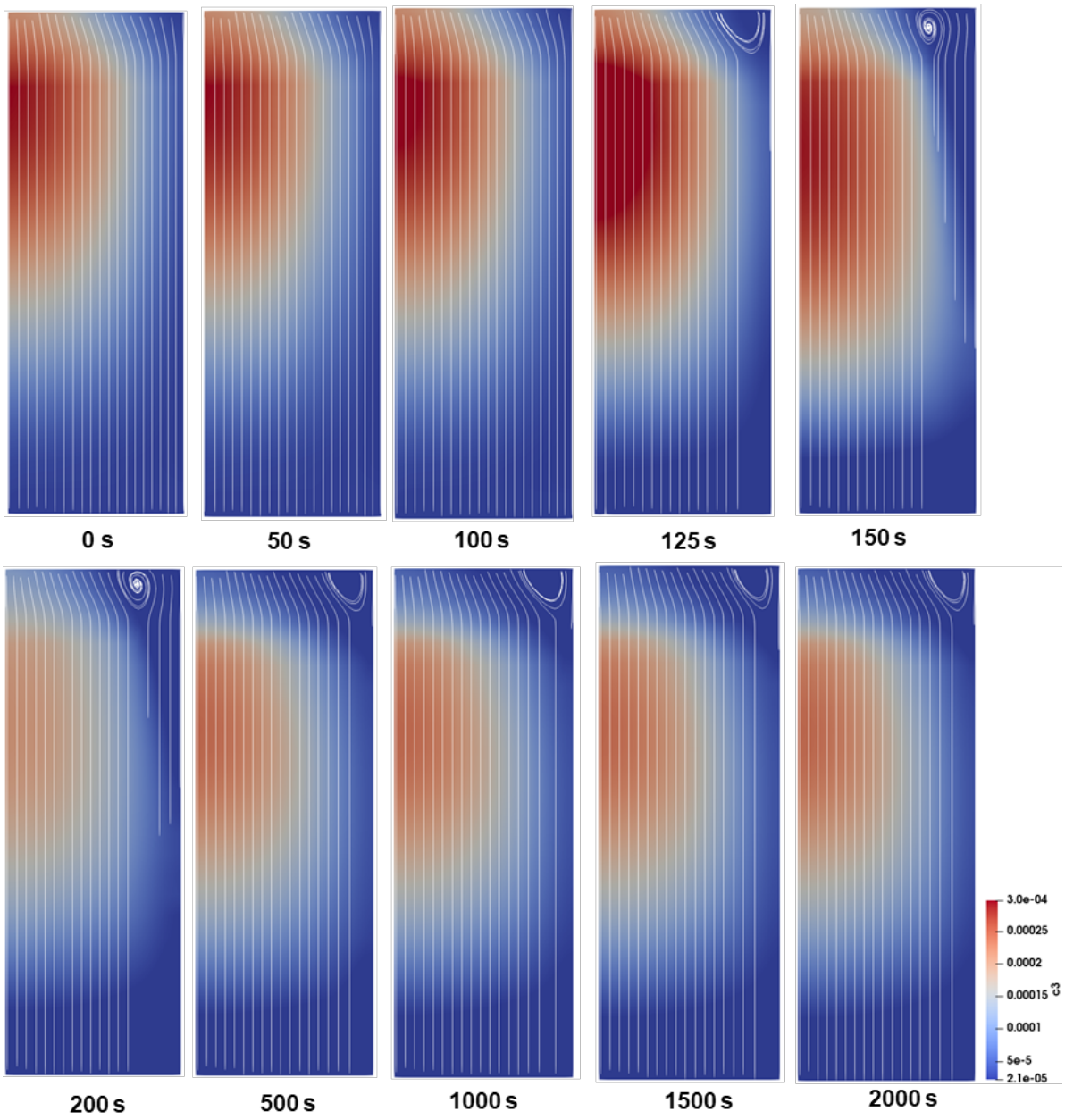

Figure 16: DNP group 3 distribution during ULOF at full power.

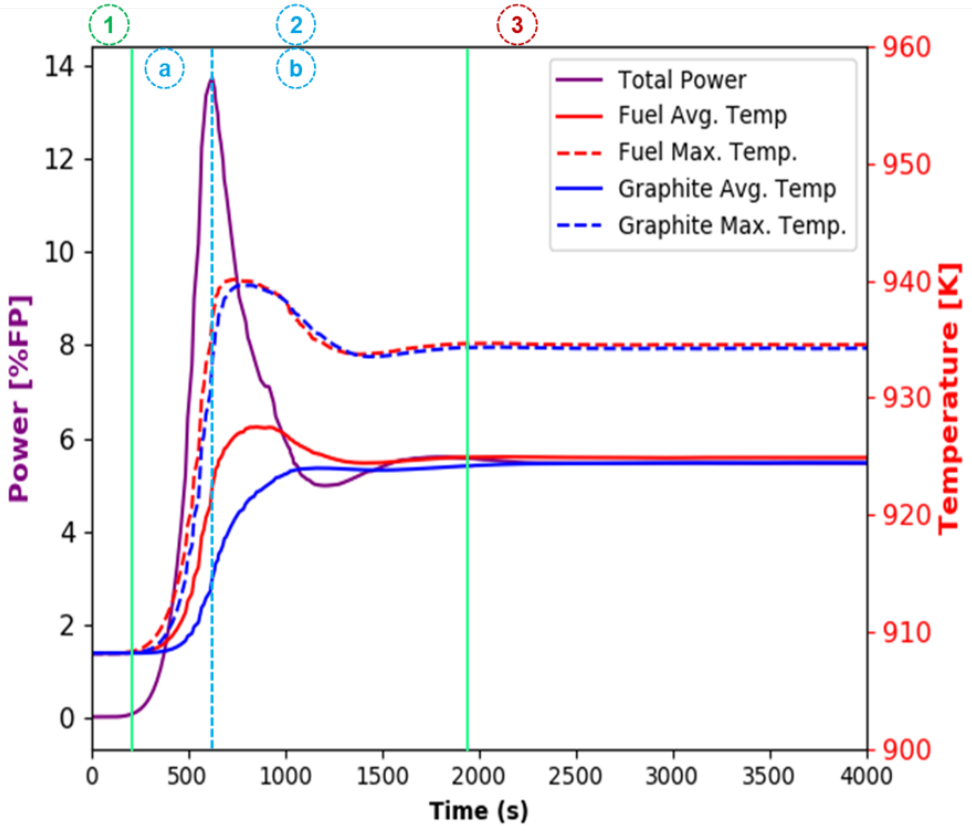

(a)

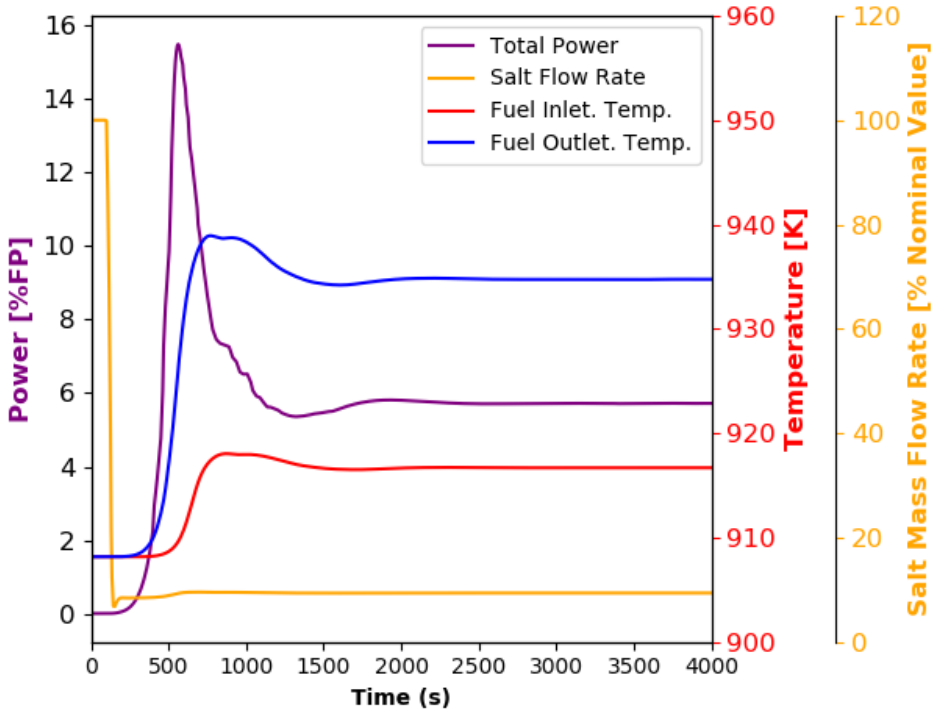

(b)

Figure 17: The MSRE ULOF transient at zero power (a) power, average fuel and moderator temperatures, (b) inlet flow rate, inlet and outlet fuel temperatures.

6. CONCLUSIONS

This report details INL's progress and activities for the NRC project "Development and Modeling Support for Advanced Non-Light Water Reactors" and reports the successful completion of one task, including:

- Task 14: MSRE model and MOOSE doc.
- Task 18: Partial requirement for task's deliverable (MSRE Report rev 0).

This report demonstrates reference plant model for the analysis of a molten salt-fueled reactor (thermal spectrum) using BlueCRAB. The fully coupled neutronics and thermal hydraulics models produced the steady state solutions of the initial core. Also, the ULOF accident scenario was simulated with the coupled neutronics and thermal hydraulics model. The effect of the DNPs drift on steady state and transient solutions were demonstrated and assessed against experimental data of the MSRE pump start-up and coast down tests at low power obtained from open literature for the purpose of validation.

Also, the ULOF accident scenario was simulated at full and zero power cases to demonstrate the impact of different feedback mechanisms of MSRs and their progression during the simulated transient. At full power operation, the negative temperature feedback dominates the positive feedback of the reduced delayed neutron losses, while the positive feedback of the reduced delayed neutron losses dominates the negative temperature feedback at low power operation. The steady state and transient solutions behaved as expected and the impact of the DNPs drift on the solutions was observed. Also, a good agreement was observed in general for pump start-up and coast down solutions, and sources of differences were identified between the current model solution and reference solution. Further improvements and modifications of the current model are suggested and discussed in Section 7.

7. FUTURE WORK

Future work should consider the following changes to improve the Multiphysics calculations:

- Improve the MSRE neutronics core model:
  - Consider a full heterogeneous model of the MSRE for accurate calculations of the DNPs drift and their corresponding reactivity losses.
  - Include the control rods in the model.
  - Include the outside regions of the active core in the MSRE model, including the core container, the downcomer, the reactor vessel, the gap between reactor vessel and insulator, the insulator, and the thermal shield.
  - Include the moderator temperature in the cross section tabulation for proper calculations of the thermal feedback.
- Improve the MSRE thermal fluids model:
  - Model the core with exact 3-D graphite core assembly geometry with fuel salt flow channels modeled with 1-D fluid components and coupled to the solid graphite region.
  - Consider the solid structures in the upper and lower plenum.
  - Model the curved shape of the upper plenum structure instead of simplified cylindrical shape.
  - Include the down comer in the core model.
  - Consider the heat generated in the graphite due to neutron slowing down and gamma heating.
  - Include a model of the tertiary loop to support modeling the natural circulation test.
- Improve and perform more validation tests of the MSRE experiments:
  - Calculate the reactivity components during transient to understand the main driving reactivity component.
  - Simulate the control rod movement during pump start-up and coast down test and compare with measured values.

  - Simulate the natural circulation test of the MSRE for validation of the model and the considered feedback mechanisms.
  - Perform more transient tests including reactivity, pump, and temperature driven transients as reactivity insertion, pump over speed, loss of heat sink, and over cooling transients.

- Model unique transients of MSRs which are important for safe operation:
  - Fuel salt over fueling transient to demonstrate the propagation and redistribution of the salt nuclides during the transient considering adding the fissile and fertile components to the salt.
  - Localized transient scenarios, specifically channel blockage and unblockage transients.

REFERENCES

[1] L. Pioro, *Handbook of Generation IV Nuclear Reactors: Introduction: Generation IV international forum, Molten Salt Fast Reactors*. Elsevier, 2016.

[2] T. Dolan, *Molten Salt Reactors and Thorium Energy: Introduction, Liquid fuel thermal neutron spectrum reactors*. Elsevier, 2017.

[3] M. Jaradat *et al.*, "Development and Validation of PROTEUS-NODAL Transient Analyses Capabilities for Molten Salt Reactors," *Annals of Nuclear Energy*, vol. 160, p. 108402, 2021.

[4] G. Yang *et al.*, "Development of coupled PROTEUS-NODAL and SAM code system for multiphysics analysis of molten salt reactors," *Annals of Nuclear Energy*, vol. 168, p. 108889, 2022.

[5] P. Balestra *et al.*, "Coupled multiphysics simulation of pool-type molten salt reactors using Griffin/Pronghorn," ANS Winter Meeting 2020, 2020.

[6] P. Balestra *et al.*, "Multiphysics Simulation of the Molten Salt Fast Reactor Using Griffin and Pronghorn," The International Conference on Mathematics and Computational Methods Applied to Nuclear Science and Engineering (MC 2021), ANS, 2021.

[7] R. Robertson, "MSRE Design and Operations Report, Part I, Description of Reactor Design," Technical Report ORNL-TM-728, Oak Ridge National Laboratory, Oak Ridge, Tennessee, 1965.

[8] M. Rosenthal, P. Kasten, and R. Briggs, "Molten-salt reactors– history, status, and potential," *Nuclear Applications and Technology*, vol. 8, pp. 107–117, 1970.

[9] P. Haubenreich and J. Engel, "Experience with the molten-salt reactor experiment," *Nuclear Applications and Technology*, vol. 8, p. 118–136, 1970.

[10] R. Briggs, "Molten-Salt Reactor Program Semiannual Progress Report," Technical Report ORNL-3626, Oak Ridge National Laboratory, Oak Ridge, Tennessee, 1964.

[11] R. Robertson *et al.*, "Conceptual Design Study of a Single-Fluid Molten Salt Breeder Reactor," Technical Report ORNL-4541, Oak Ridge National Laboratory, Oak Ridge, Tennessee, 1971.

[12] R. Thoma, "Chemical aspects of MSRE operations," Technical Report ORNL-4658, Oak Ridge National Laboratory, Oak Ridge, Tennessee, 1971.

[13] R. Kedl, "Zero-Power Physics Experiments on the Molten-Salt Reactor Experiment," Technical Report ORNL-4233, Oak Ridge National Laboratory, Oak Ridge, Tennessee, 1968.

[14] R. Steffy, "Inherent neutron source in MSRE with clean 233U fuel," Technical Report ORNL-TM-2685, Oak Ridge National Laboratory, Oak Ridge, Tennessee, 1696.

[15] R. Kedl, "Fluid Dynamic Studies of The Molten-Salt Reactor Experiment (MSRE) Core," Technical Report ORNL-TM-3229, Oak Ridge National Laboratory, Oak Ridge, Tennessee, 1970.

[16] C. Permann *et al.*, "MOOSE: Enabling massively parallel multiphysics simulation," *SoftwareX*, vol. 11, no. 10, p. 100430, 2020.

[17] D. Gaston *et al.*, "Physics-based multiscale coupling for full core nuclear reactor simulation," *Annals of Nuclear Energy*, vol. 84, pp. 45–54, 2015.

[18] R. Martineau, "The moose multiphysics computational framework for nuclear power applications: A special issue of nuclear technology," *Nuclear Technology*, vol. 207, no. 7, pp. iii–viii, 2021.

[19] Y. Wang *et al.*, "Rattlesnake: A moose-based multiphysics multischeme radiation transport application," *Nuclear Technology*, vol. 207, no. 7, pp. 1047–1072, 2021.

[20] F. Gleicher *et al.*, "The coupling of the neutron transport application RATTLESNAKE to the fuels performance application bison," in *International Conference on Reactor Physics (PHYSOR 2014)*, (Kyoto, Japan), May 2014.

[21] Y. Jung and C. Lee, "PROTEUS-MOC User Manual," Technical Report ANL/NE-18/10, Argonne National Laboratory, September 2018.

[22] P. Romano *et al.*, "OpenMC: A State-of-the-art Monte Carlo Code for Research and Development," *Annals of Nuclear Energy*, vol. 82, pp. 90–97, 2015.

[23] M. Jaradat, *Development of Neutronics Analysis Capabilities for Application of Flowing Fuel Molten Salt Reactors*. PhD thesis, University of Michigan, 2021.

[24] M. Chadwick *et al.*, "ENDF/B-VII.1: nuclear data for science and technology: cross sections, covariances, fission product yields and decay data," *Nuclear Data Sheets*, vol. 112, p. 2887–2996, 2011.

[25] M. Aufiero *et al.*, "Calculating the effective delayed neutron fraction in the Molten Salt Fast Reactor," *Annals of Nuclear Energy*, vol. 65, p. 78–90, 2014.

[26] R. Hu *et al.*, "SAM theory manual," Tech. Rep. ANL/NE-17/4 Rev.1, Argonne National Laboratory, 2021.

[27] G. Yang *et al.*, "Updated SAM Model for the Molten Salt Reactor Experiment (MSRE)," Tech. Rep. ANL/NSE-23/8, Argonne National Laboratory, 2023.